Title
THE EFFECT OF SURFACE DOPING ON THE OXIDATION OF CHROMIA FORMER ALLOYS

Author
Landkof, M.

Publication Date
1984-04-01

Lawrence Berkeley Laboratory
UNIVERSITY OF CALIFORNIA

Materials & Molecular Research Division

Presented at the Annual Meeting of the National Association of Corrosion Engineers, Corrosion 84, New Orleans, LA, April 2, 1984; and submitted to Corrosion

THE EFFECT OF SURFACE DOPING ON THE OXIDATION OF CHROMIA FORMER ALLOYS

M. Landkof, D.H. Boone, R. Gray, A.V. Levy, and E. Yaniv

April 1984

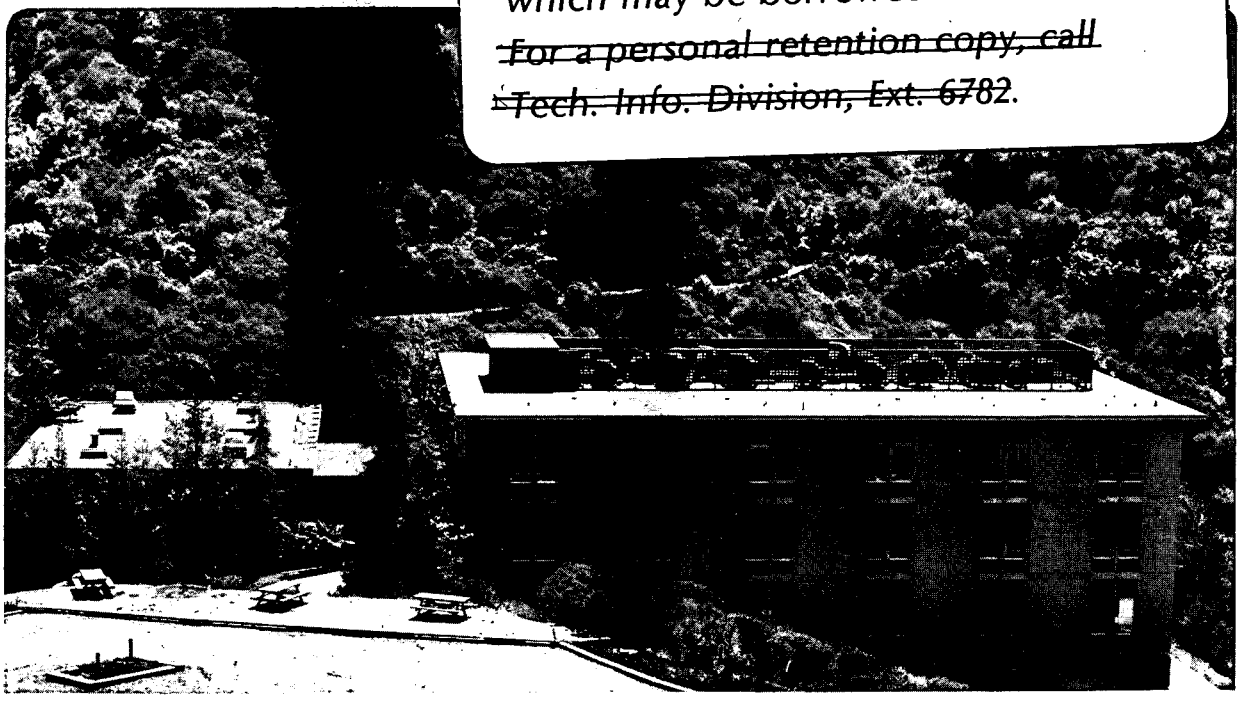

Prepared for the U.S. Department of Energy under Contract DE-AC03-76SF00098

DISCLAIMER

LBL-17237

THE EFFECT OF SURFACE DOPING ON THE OXIDATION OF CHROMIA FORMER ALLOYS

M. Landkof, D. H. Boone, R. Gray, A. V. Levy, E. Yaniv

Materials and Molecular Research Division
Lawrence Berkeley Laboratory and
Department of Materials Science and Engineering
University of California
Berkeley, California 94720

Research sponsored by the Department of Energy under DOE/FEAA 12 10 10 0, Advanced Research and Technical Development, Fossil Energy Materials Program, Work Breakdown Structure Element LBL-3.5 and under Contract No. DE-AC03-76SF00098

ABSTRACT

The influence of the surface application of active elements (doping) on the composition, morphology, adherence and the growth rate of oxide scales formed during exposure to high temperature has been investigated. The active elements were applied as aqueous solutions of nitrate salts which were subsequently transformed to oxide. The active elements used were: Y, Ce, La, Hf, Ca, and Zr. The chromia forming substrates used were type 304 and 310 stainless steels and IN 738, a nickel base alloy. In order to determine the effect of the minor alloying elements in stainless steels on the surface doping effect, Y was applied to three alloy modifications of type 304SS. The presence or absence of Mn and Si in the alloy on the high temperature corrosion behavior was determined. Several different doping techniques were used to determine which technique was most beneficial to the behavior of the oxide barrier scale.

The application of Y, Ce and La was found to enhance the oxidation resistance of the commercial stainless steels while no benefits were found for alloys doped with Hf, Ca and Zr. It was determined that Si had to be present in the type 304SS for the doping process to enhance the oxidation resistance. There was no beneficial effect on modified 304SS containing Mn only or without Mn or Si. The yttrium doped and undoped modified type 304SS with Si only showed more resistance to scale spallation than any other type 304SS alloy tested, either commercial or modified.

INTRODUCTION

The beneficial effects of active elements additions (doping) on the oxidation resistance of many heat resistant alloys are well known.[1-10] The major improvements that have been observed are: better adherence of the scale to the substrate, slower rates of oxidation (particularly for Cr_2O_3 formers), and higher Cr_2O_3 contents in the oxide scale. Although there is no generally accepted theory, some explanations have been offered for these improvements. The oxygen active elements may act as scale nucleation sites, reducing the distance between the chromia crystal nuclei which shortens the transient stage of oxidation and produces a continuous protective scale earlier that has a smaller oxide grain size.[8,9,10] The better adherence may be caused by lower growth stresses in the scale as a result of a slower oxidation rate, by easier accomodation of the scale growth and resultant thermal stresses because the finer grain size scale is more plastic, or by the active element oxide promoting mechanical keying of the scale to the substrate (pegging).[10]

It has been suggested that the reduction of the oxidation rate of the doped alloys may be a result of blocking or removing of short circuit diffusion paths (thought to be dislocations networks) for cations.[5] In the extreme case the oxide forming reaction may move from the oxide-oxygen interface to the oxide-alloy interface, making the slower transport process of inward oxygen diffusion rate controlling. This change in mechanism would also decrease or even eliminate void formation at the oxide-alloy interface which would also improve adherence.

Up to the present, most effort has been concentrated on internal doping, the active elements being added directly to the alloys as a metallic or dispersed oxide. However, one of the original patents[2] on active element addition suggested direct surface additions by application of solutions of a salt of the active element on the metal surface. Some attempts at ion implantation of the active element into the surface region have also been carried out.[11]

External doping of chromia former alloys is an important means of alloying because of its possible commercial advantages which include:

1. low cost
2. simplicity
3. relatively little time used in the doping process
4 no major adverse effects on the material's mechanical properties as can occur with internal doping

The purpose of this work was to examine the possibility of applying the active element via the aqueous solution approach to achieve these advantages.

The investigation was divided into two parts. The first part investigated the effects of doping type 304SS, type 310SS and IN 738 with different active elements. A number of different doping elements were tried, all having very high negative free energies of oxide formation. Three commercial alloys were chosen with different propensities to form complete chromia layers under conditions of high temperature air oxidation without doping. Type 304SS has a borderline Cr content (18%) and does not form a continuous external chromia layer without doping. The doping resulted in the formation of a continuous

chromia layer. The type 310SS with a higher Cr content (25%) is able to form a continuous chromia layer under normal conditions and the principal effects of the doping were postulated to be modification of the oxide scale morphology, its adherence and the oxidation rate. The IN 738, a nickel base alloy requires less Cr content to form a continuous scale than the iron base, austenitic stainless steels. Five doping solutions, and two doping methods, were evaluated to determine which enhanced the oxidation resistance the most. The second part of the experiment determined the role of the minor alloying elements Mn and Si on the high temperature spallation resistance of yttrium doped type 304SS.

The best doping solution and method determined in the first part of the investigation was used in the second part to study their effects on four different type 304SS compositions.

EXPERIMENTAL PROCEDURE

The nominal compositions of the commercial alloys used in the investigation are listed in Table (1a). Coupon specimens, 15mm x 10mm x 2mm, were final polished on a 600 grit SiC paper, ultrasonically cleaned in ethanol and dried.

A number of pure and commercial 304SS samples were doped using the various methods described in Table 2 to determine which method to select for the balance of the experiments. The dopants used are listed in Table 1B. Of the five doping methods, see Table 2, the 'wet' and 'wet + dry' had the poorest results while the 'hot,' 'dry' and 'spray' methods all gave acceptable results. The 'hot' method was chosen as the best method because it was felt that the deposition of yttrium on a

hot surface would be more uniform than allowing the aqueous salt solution to stand for a long while in air at room temperature while it dried. Even so, the hot doping method produced some non-uniformities in YNO_3 depositions, see Figure 1. The spray method was not chosen primarily because it proved unwieldly using the simple equipment available. It was found that the addition of HNO_3 to the 10% YNO_3 solution to achieve a pH=2 was crucial to attaining any consistently positive results.

The doped specimens were oxidation tested in air either isothermally at 1000°C for 50 hr or by thermally cycling them for 20 hr cycles at 1000°C, cooling to room temperature between each cycle. The oxidized specimens were examined using standard metallographic techniques and the scanning electron microscope (SEM) and scanning Auger microscope (SAM). The oxides that did not spall were stripped off by dipping the specimens in a 10% bromine-methanol solution so that the scale could be isolated from the substrate for analysis.

The modified type 304SS specimens were prepared by melting a 500g ingot of the desired composition in a vacuum induction furnace, rolling the ingot into a sheet approximately 3mm thick, and cutting 10 x 15mm coupons from the sheet. All coupons were ground to 120 grit and ultrasonically cleaned in ethyl alcohol for 15 minutes.

The modified alloy compositions and the abbreviations used to identify them are:

1.	comm (commercial)	Fe-18Cr-8Ni-2Mn-1Si
2.	+Si	Fe-18Cr-8Ni-1Si
3.	+Mn	Fe-18Cr-8Ni-2Mn
4.	pure	Fe-18Cr-8Ni

RESULTS

1. DOPED COMMERCIAL ALLOYS

Isothermal Oxidation (50hr at 1000°C)

The samples after oxidation are shown in Figure 2. Y, Ce and La doping prevented spalling of the oxide scale. The oxides on the Zr, Hf and Ca doped samples spalled off to about the same degree as occurred on the undoped type 304SS samples. The adherent scale formed on the Y, Ce and La doped specimens had a dark green-gray color typical of Cr_2O_3. The scale which spalled off from the undoped, and the Zr, Hf and Ca doped specimens had a dark blue color on the outer surface and was brown on the under surface, indicating a graded composition.

Cross sections of the Y, Ce and La doped specimens and the undoped 304SS were prepared and studied in the SEM. In Figure 3 a cross-section of the undoped scale in an area where it remained adherent is shown. This scale is thick (25μm) and appears to be a spinel ($FeCr_2O_4$). In Figure 4 the cross section of the Y doped scale is shown, This scale is about 1/5th the thickness of the scale on the undoped specimen and is Cr_2O_3. Iron could be detected in the scale using the energy dispersive x-ray analysis system (EDAX) attached to the SEM.

In Figure 5 the cross section of the Ce doped scale is shown. This scale is thicker than that of the Y doped scale but is still much thinner than that of the undoped type 304SS. The scale consisted primarily of Cr_2O_3 but some isolated areas rich in iron oxide were detected in the scale.

The Y, Ce and La doping of the type 304SS surface resulted in the formation of more adherent, Cr rich, oxide scales. The spalled scales of the Hf, Zr and Ca doped specimens were not analyzed in the SEM. However, their color and appearance was so similar to the spalled scale of the undoped type 304SS that their structure and composition can be expected to be of the same type as that observed in Figure 3 on the undoped alloy, a graded iron chromate.

The unspalled scale on the yttrium doped specimen was stripped off with a 10% bromine-methanol solution and analyzed in the SEM +EDAX. The spalled pieces of the undoped scale were also studied. The outer surface of the doped scale was composed primarily of chromia containing a small amount of manganese and was in small dia (<3μm) crystallites that are highly convoluted, see Figure 6. On the under surface of the scale, webs of SiO_2 were observed in addition to the Cr_2O_3, see Figure 7.

The spalled pieces of oxide (Figure 8) from the undoped alloy were almost pure iron oxide in the high protrusions on the outer surface with some Mn (probably in the form of $MnFe_2O_4$) in the continuous oxide scale between the protrusions. The under surface of the scales was Cr rich with quite high amounts of iron (probably Cr_2O_3 + $FeCr_2O_4$), noticeable amounts of Si (SiO_2) in a web configuration apparently

conforming to the base metal grain boundaries, and some Ni ($NiCr_2O_4$). Precise compound compositions and structures, however, were not identified. There was no indication of oxide pegs in the doped scale to account for the adherence as occurs in some alloys with internally added active elements.

Cycling Oxidation (20hr at 1000°C - per cycle)

Table 3 summarizes the results of the thermal oxidation tests. The yttrium doped surface underwent the most thermal cycles before spalling began to occur.

2. YTTRIUM DOPED ALLOYS - ISOTHERMAL OXIDATION

Type 304SS Alloy

The most pronounced effect of surface active element doping with Y was observed on the type 304SS alloy. The doping affected the adherence, the thickness, the composition and the morphology of the oxide scale formed. The doped scale did not undergo any spallation after seven cycles (20 hr at 1000°C each cycle) while the scale on the undoped alloy spalled on the first cycle. The average thickness of the scale on the doped alloy was about 5μm (Figure 4) and for the undoped alloy, 25μm, in areas where part of the scale remained attached to the alloy surface (Figure 3). Some of the spalled pieces from the undoped alloy were even thicker. The results are presented in Table 4.

Type 310 Alloy

The oxide scale formed on the Y doped sample was thinner than the scale on the undoped specimen, Figure 9. As shown in Figure 10 the

outer surface of the scale is composed of tightly packed, convoluted crystallites similar to those seen on the outer surface of the Y doped type 304SS scale, Figure 6. On the undoped type 310SS the Cr_2O_3 crystallites are non-uniform in size and shape, see Figure 11. No noticeable differences could be detected in the adherence and the chemical composition of the oxide scale formed on the Y doped and the undoped 310SS specimens. The results are summarized in Table 5.

IN 738 Alloy

Some differences were found between the yttrium doped and the undoped IN 738 alloy specimens. The scale thickness was 7 - 9μm on the Y doped sample and 10 - 12μm on the undoped samples and the morphology of the internal oxidation layer differed,see Figure 12. The darker areas of internal oxidation are rich in Al. They are longer and more continuous in the undoped sample. The external layer is almost pure Cr_2O_3 with some Ti in it.

The outer surface of the scale on the yttrium doped specimen has a slightly finer crystalline structure than that on the undoped specimen. Some non-uniform growth can be seen on the undoped sample,Figure 13. The very thin translucent film areas that can be seen on the doped sample are rich in Y and are the remains of the external Y doping solution. It can be seen that the general nature of the morphology of both scales is similar. The oxidation test results are summarized in Table 6.

Active Element Distribution in the Scale

Some analysis of surface composition distribution was done using

the scanning Auger microscope (SAM) to define the location of the dopant element yttrium during the various stages of nitrate decomposition and oxidation of type 304SS. After the decomposition stages (1/2 hr at 500°C) yttrium could be readily detected in the surface film, see Figure 14. No nitrogen was detected and it may be assumed that the decomposition stage was complete. The thin film (800Å) was mostly Y_2O_3 with some chromium and iron oxide formed near the scale-metal interface. After a short oxidation period at high temperature (15 min at 1000°C), the yttrium could barely be detected, see Figure 15. A high Cr content in the scale indicates Cr_2O_3. Some manganese oxide was found on the top of the scale. The 1000°C temperature probably promoted an initial preferential oxidation of Cr and Mn because of their higher diffusion rates. However, the absence of iron oxide even after longer oxidation times cannot be solely explained by this enhanced diffusion. Iron oxides were observed on the undoped type 304SS after long oxidation times. The presence of yttrium could be affecting the formation of iron oxide.

3. DOPED EXPERIMENTAL ALLOYS

The test series carried out to determine the role of minor alloying elements in commercial type 304SS on the surface doping behavior of the alloy involved only manganese and silicon contents. The qualitative results of the thermal tests run on the modified alloys are summarized in Tables 7, 8 and 9. These tables show that the yttrium doped alloys without Si (+Mn and pure) had no increased corrosion resistance with respect to undoped type 304SS. These samples rarely remained in the non-spalled condition for even an hour at

1000°C, Figure 16. The spalled scale from these samples was primarily Fe_2O_3 as determined by x-ray diffraction. A cross sectional view and x-ray maps of the +Mn (no Si) modified type 304SS sample showing the lack of a chromia scale after spallation can be seen in Figure 17.

The commercial type 304SS yttrium doped samples containing both Si and Mn and used as a control in these thermal tests behaved approximately as reported in section 1 above. The adhered scale color was green-gray and was composed of Cr_2O_3, Fe_3O_4, and Y_2O_3. The samples' average number of cycles to spalling was eight 20 hour, 1000°C cycles.

The yttrium doped +Si 304SS (no Mn) showed increased spallation resistance compared to the commercial type 304SS. Samples were cycled twenty times to 1000°C and heated isothermally at 1000°C for 42 days with no signs of spallation. The scale color changed from light green at the beginning of the tests to a darker green towards the end. Scale compostition consisted of Cr_2O_3, Y_2O_3, and $YCrO_3$ as determined by x-ray diffraction. Cross section pictures and x-ray maps of this type of sample in Figure 18 show a protective chromia scale.

The undoped +Si 304SS (no Mn) showed increased resistance to spallation compared to the commercial type 304SS. Samples completed twenty 20 hour cycles to 1000°C with no spallation. The scale was battleship grey in color and was composed of Cr_2O_3 as determined by x-ray diffraction. Figure 19 shows the superior spalling resistance of doped +Si 304SS (no Mn) as compared to doped comm. 304SS (Si+Mn). Undoped and doped +Si 304SS (no Mn) had equal resistance to spallation within the limits of the experiments.

DISCUSSION

1. Method of Applying the Doping Element

Several details of the doping method were determined to be critical to the success of the process. The overall variables in the process that were investigated are present in Table 2. In this section, some of the important process details are highlighted.

The purpose of heating the samples before dipping them into the active element nitrate solution is to form a thin oxide scale that would improve the wetting properties of the surface and thus produce more uniform distribution of the nitrate. The application technique seems to influence the protectivity of the doped scale. When the "hot" doping technique specimens were tested the change from a greenish to a reddish color appeared on the surface after the fourth thermal cycle, (20 hr at 1000° per cycle), indicating iron diffusion outward. When the sample was painted or dipped after first being allowed to cool from the thin oxide formation step, the iron diffusion color change occurred earlier, after the second thermal cycle. The reason for better barrier performance in the first case may be in the better incorporation of the doping salts into the initial thin oxide scale.

The salt decomposition heating stage (1/2 hr at 500°C) after application of the salt is to decompose the nitrate salts. Because no nitrogen was detected in post application surface chemical analysis, it may be assumed that the decomposition was completed. This salt decomposition, if done simultaneously with high temperature oxidation (1000°C) could interfere with the oxide growing process as nitrogen

oxides could form that might degrade the protective oxide barrier. The depth of yttrium penetration as an oxide in the doped type 304SS alloy after the transformation stage at 500°C was observed to be 800Å. Transformation carried out at a lower temperature, 200°C, resulted in the formation of a slightly thinner protective scale during the subsequent 1000°C oxidation.

Although the enhanced protection from a single application of an active element salt occurred for only 8 thermal cycles maximum, it appears that the effect may be prolonged by additional applications of the doping element. It was found that by reapplying the yttrium nitrate after the third thermal cycle very slight spallation appeared only after 13 thermal cycles. Additional studies of this behavior are planned.

2. Different Doping Elements on 304SS

Y, Ce and La as dopants were found to be very beneficial to the formation and behavior of the barrier scale, with the most pronounced effect occurring on the type 304SS. The doping affected the formation rate, composition and morphology of the oxide scale and appeared to increase its adherencey. The application of Ce and La was slightly less effective than Y. Some iron was found in the Ce and La doped scales while none occurred in the Y doped scale. The Ce and La doped scales were also thicker and were less adherent on thermal cycling than the scale formed on the Y doped specimens.

The beneficial affect of Y, Ce and La surface additions on the performance of the oxide protective barrier scales on Cr_2O_3 scale forming alloys is thought to be primarily due to their promotion of

scale nucleation sites. The proliferation of sites decreases the distance between the stable, chromia forming nuclei during the early stages of oxidation which results in a smaller oxide grain size. Also, the surface is completely covered by the protective chromia layer at an earlier time.[5] The smaller grain size may also improve the adherence of the scale by making it more deformable during its growth period and during thermal cycling when it deforms by sliding along grain boundaries.[10] Figures 20 and 21 graphically depict the scale nucleation and growth mechanisms in undoped and doped type 304SS.

The slower oxidation rate which results in a thinner oxide scale may be explained by the theory developed by J. Stringer,[5] He proposed that the doping element's oxides block the short circuit paths for cation diffusion (diffusion along dislocations). In the most extreme case this may cause a change of the oxide formation mechanism from an outward, cation diffusion type to an inward, oxygen, anion diffusion type. In the anion diffusion case, less voids form at the metal-oxide interface which could aid scale adherence.[5,10] The behavior is quite similar to that obtained by internal doping of the alloys.[3]

The poor behavior of Hf and Zr externally doped scales was unexpected. Hf and Zr internal alloying additions are known as being beneficial.[8] The absence of an active element effect when these elements are applied by external means may be explained by the anisotropic nature of their oxides. This behavior can be more important for external doping of the alloys than for internal doping, especially for the initial stages of oxidation. The thermal expansion along one of the crystallographic axes of HfO_2 and ZrO_2 is extremely

low see Table 10. Also the total polycrystalline thermal expansion of ZrO_2 and HfO_2 in the monoclinic form is somewhat lower than that of the Y, Ce and La oxides, making them more incompatible with the higher thermal expansion base metals. It is well known that oxides such as Y_2O_3 and MgO are added to sprayed ZrO_2 coatings on metals to stabilize the cubic structure[8] which increases the total linear thermal expansion of the ZrO_2 to make it more compatible with its metal substrate.

The general spallation of the Ca doped sample in the first thermal cycle can be explained by the low melting eutectic that CaO forms, especially with Cr_2O_3, Table 11 at the test temperature. The closer the working temperature is to the melting point of the oxide, the higher is the possibility of oxygen transfer to the metal-oxide interface which deteriorates the scale-metal bond.

3. Other Commercial Chromia Former Alloys

The type 310SS with 25% Cr and the IN 738 alloy containing Ni and Cr form a complete chromia barrier scale layer more readily without any additives than the type 304SS does. The active element doping of these alloys, therefore, did not have as marked an effect on the ability to form a good barrier oxide scale at 1000°C as occurred on the 304SS. However, some improvement in the scale morphology and the oxidation rate was observed. The non-uniform growth of the oxide scale on the undoped samples in comparison to the uniform growth of the scale on the doped samples supports the postulation that the doping elements provide nucleation sites during the early period of the oxidation reaction. There also may have been some influence of the doping on adherence

during thermal cycling.

4. Effect of Si and Mn in 304SS

The beneficial effect of the presence of Si in the type 304SS is thought to be due to the formation of the Si rich webs which form at the scale-metal interface along the metal's grain boundries. The webs cause an increase in the scale-substrate adhesion. Exactly how the doping relates to the SiO_2 web formation is not known.

The beneficial effect of the absence of Mn in the type 304SS is thought to be due to the absence of the less dense spinel, $MnCr_2O_4$. Many spinels are noted for their stress concentrating effects. When these stresses are sufficient to crack open the scale, they can cause new cation/anion diffusion paths to occur. These new short circuit diffusion paths allow the inward diffusion of oxygen to the substrate and outward diffusion of Fe to the scale-atmosphere interface, thereby deteriorating the barrier scale. Because of the absence of these effects without Mn in the alloy, the Fe_2O_3 phase does not form and the scale is more adherent.

CONCLUSIONS

1. Surface doping of type 304SS with some active elements that have high negative free energies for their oxide formation enhances corrosion resistance at 1000°C.

2. Yttrium and to a lesser extent lanthanum and cerium enhance oxidation resistance while hafnium, zirconium and calcium do not.

3. Yttrium oxide causes earlier nucleation of Cr_2O_3 resulting in:
   - o better adherence of scale
   - o thinner scale
   - o smaller grain size of scale
   - o more uniform scale morphology
   - o different scale composition (Cr_2O_3 not Fe_2O_3)
   - o blocking of diffusion paths for oxygen in scale

4. Oxide scale on 310SS oxide scales are not helped as much as those on type 304SS by external doping with active elements.

5. Si is required in type 304SS in order for external doping to enhance its scale adherence and corrosion resistance. This is due to the presence of SiO_2 webs at the scale-metal interface.

6. Yttrium doping of type 304SS without Si has no added benefit to its high temperature corrosion resistance.

7. The absence of Mn in type 304SS, without doping, improves its high temperature corrosion resistance significantly.

8. The high temperature corrosion resistance of doped and undoped type 304SS without Mn are approximately the same.

Research sponsored by the U.S. Department of Energy under DOE/FEAA 12 10 10 0, Advanced Research and Technical Development, Fossil Energy Materials Program, Work Breakdown Structure Element LBL-3.5 and under Contract No. DE-AC03-76SF00098.

REFERENCES

1. L. B. Pfeil 1937 U.K Patent No. 459484.

2. L. B. Pfeil 1947 U.K. Patent No. 574088.

3. J. M. Francis and W. H. Witlow Corros. Sci., Vol. 5,p 701 (1965).

4. C. Wood and J. Boustead, Corros. Sci. Vol.8,p. 719 (1968).

5. J. Stringer, B. A. Wi.cox and R. I. Jaffe, Oxid. of Met. Vol.5,p. 11 (1972).

6. I. G. Wright and B. A. Wilcox, Oxid.of Met. Vol.8,p. 283 (1974).

7. F. A. Golighty, G. H. Stott and G. C. Wood, Oxid.of Met. Vol.10,p. 193 (1976).

8. D. P. Whittle, M. E. El-Dahshan and J. Stringer, Corr. Sci. Vol.17,p. 879 (1977).

9. I. M. Allam, D. P. Whittle and J. Stringer, Oxid. of Met. Vol. 13,p. 381, (1979).

10. D. P. Whittle and J. Stringer, Phil, Trans. R. Soc. Lond. Vol.A295,p. 309 (1979).

11. J. E. Antill, J. J. Bennet, R. F. A. Bearnaley, F. H. Fern, P. H. Goode, B. L. Myatt, J. F. Furner and J. B. Warburton, Corros. Sci. Vol.16, p. 729 (1976).

12. J. C. Touloukian, R. K. Kirby, R. F. Taylor and T. Y. Lee, Thermo physical Properties of Matter, The TPRC Data Series, vol. 13- Thermal Expansion of Metallic Solids.

13. J. Kuminik Jr. High Temperature Inorganic Coatings, Reinhold Pub. (1983).

FIGURE CAPTIONS

1. Yttrium doped 304SS showing non-uniformities of surface morphology at different places along the sample.

2. 304SS alloy doped with different active elements after isothermal oxidation.

3. Cross section of the 304SS undoped sample oxidized for 50 hours at 1000°C in air.

4. Cross section of the 304SS yttrium doped sample oxidized for 50 hours at 1000°C in air.

5. Cross section of the 304SS cerium doped sample oxidized for 50 hours at 1000°C in air.

6. Outer surface of 304SS yttrium doped oxide scale removed from the substrate.

7. Under surface of the 304SS yttrium doped oxide scale removed from the substrate.

8. Outer (a) and under (b) surface of the 304SS undoped, spalled off oxide scale.

9. Cross section of the 310SS yttrium doped and undoped samples oxidized for 50 hours at 1000°C in air.

10. Outer surface of the 310SS yttrium doped oxide scale.

11. Outer surface of the 310SS undoped stripped off oxide scale.

12. Cross section of the 738 Inconel alloy yttrium doped and undoped samples oxidized for 50 hours at 1000°C in air.

13. Outer surface of the IN 738 yttrium doped (a) and undoped (b) stripped off oxide scale.

14. SAM composition profile through the oxide scale on 304SS yttrium doped sample after the preoxidation stage (30 min. at 500°C). Sputtering rate 400 A/min.

15. SAM composition profile through the oxide scale formed on 304SS yttrium doped sample after the preoxidation (30 min. at 50°C) + oxidation (15 min. at 1000°C) stages. Sputtering rate 400 A/min.

16. Yttrium doped alloy modifications of 304SS shown after oxidation exposure.

17. Cross section of modified (with Mn without Si) 304SS in the spalled condition.

18. Cross section of modified (with Si without Mn) 304SS in the unspalled condition.

19. Samples showing the increased high temperature spallation resistance of doped +Si 304SS (no Mn) compared to doped commercal 304SS (Mn+Si).

20. Proposed corrosion mechanism of undoped commercial 304SS.

21. Proposed corrosion mechanism of yttrium doped commercial 304SS

Table 1A - Composition of Commercial Alloys Investigated

	Fe	Cr	Ni	Mn	Si	Co	Mo	Ti	Al	W	Zr	C	P	S
304SS	bal.	18.00/ 20.00/	8.00/ 10.50	2.00	1.00							.08	.045	.030
310SS	bal.	24.00/ 26.00	19.00/ 22.00	2.00	1.50							.25	.045	.030
IN738		16.00Bal.		.2	.3	8.5	1.75	3.4	3.4	2.6	.1	.17		

Table 1B - Active Elements' Nitrates Used

Nitrate	Produced by Producer
$Y(NO_3)_3.6H_2O$	Orion
$Ce(NO_3)_3.6H_2O$	"
$La(NO_3)_3.6H_2O$	Ventura Corp.
$ZrO(NO_3)_2.H_2O$	Noah
$Hf(NO_3)_4.XH_2O$	"
$Ca(NO_3)_2.4H_2O$	Orion

Table 2

APPLICATION METHODS

	PROCEDURES	COMMENTS
"Wet" doping	1. Grind to 120 grit 2. Ultrasonically clean in ethyl alcohol 15 min. 3. Detergent washed until a continuous film of water appears on the surface 4. Rinse copiously in distilled water 5. Soak in YNO_3 solution for ½ hour 6. Blot off excess solution 7. Dry in room temperature 8. Heat for ½ hour at 500°C	Unsatisfactory method
"Dry" doping	1. Grind to 120 grit 2. Ultrasonically clean 3. Heat in air 500°C for 5 min. 4. Cool to room temperature 5. Dip in YNO_3 for 5 min. 6. Blot off excess solution 7. Air dry 8. Heat at 500°C for ½ hour	Satisfactory method but method not used as hot doping method proved to be better
"Wet & Dry" doping	1. Grind to 120 grit 2. Ultrasonically clean 3. Detergent wash until continuous film of water appears on surface 4. Rinse copiously with distilled water 5. Dip in YNO_3 solution for ½ hour 6. Blot off excess solution 7. Dry in air at room temperature	Too extensive a procedure for the results obtained

Table 2 (cont'd)

	PROCEDURES	COMMENTS
"Wet & Dry" doping	8. Heat at 500°C for 5 min. 9. Cool to room temperature 10. Dip in YNO_3 solution for 5 min. 11. Blot off excess solution 12. Dry in air 13. Heat at 500°C for ½ hour	
"Hot" doping	1. Grind to 120 grit 2. Ultrasonically clean 3. Heat to 500°C for 5 min. 4. Quickly place specimen in YNO_3 solution directly after taking out of furnace 5. Leave specimen in solution just past the flash point 6. Blot off excess solution 7. Dry in air at room temperature 8. Heat to 500°C for 5 min.	Method was used for the balance of the experiments
"Spray" doping	1. Grind to 120 grit 2. Ultrasonically clean 3. Heat to 500°C for 5 min. 4. Spray with YNO_3 solution while still hot 5. Blot off excess solution 6. Dry in air at room temperature 7. Heat to 500°C for 5 min.	Satisfactory method but not used

Table 3 Cyclic Oxidation of 304 SS (20 hr. Cycles at 1000°C)

ELEMENT DOPED	CYCLE 1	CYCLE 2	CYCLE 3	CYCLE 4	CYCLE 5	CYCLE 6	CYCLE 7	CYCLE 8
Undoped	General spallation							
Hf	General spallation							
Ca	General spallation							
Zr	Beginning of spallation	General spallation						
Ce	Very small spots of spallation Greenish gray color	No change	No change	Start of general spallation	Increase in spallation with swollen areas	Further increase in spallation with more swollen areas		
Y	No spallation Greenish gray color	No change	No change	Color change to brownish red. No spallation	No change	No change	More brownish red color	Start of spallation, especially on the specimen edges
La	No spallation Greenish gray color	Start of general spallation						

Table 4

SCALE DESCRIPTION

	304 SS Y Doped	304 SS Undoped
Spallation	No spallation detected after 50 hr. oxidation in air at 1000°C	General Spallation occurred after 50 hr. oxidation in air at 1000°C
Thickness	2-5 μm continuous layer	Thick, up to 40 μm
Composition	Almost pure Cr_2O_3 with some $Mn(MnCr_2O_4)$ on the under side. SiO_2 distribution along apparent alloy grain boundaries	Almost pure iron oxide on the outer surface and mixed FeCr oxides under surface with some Ni and Mn incorporated
Morphology	Uniformly grown groups of small crystallites	Nonuniform structure. High protrusions of iron oxide

Table 5

SCALE DESCRIPTION

	310 Y Doped	310 Undoped
Spallation	No spallation detected after 50 hr oxidation in air at 1000°C.	No spallation detected after 50 hr oxidation in air at 1000°C.
Thickness	Thin scale	Thicker scale 5-8 μm. Examining the surface revealed scale free areas which probably form during lifting and cracking of the scale.
Morphology	Uniform growing, small crystallites of uniform size. The small crystals are very tightly packed.	Nonuniform growing crystallites of different sizes. Loosely bonded crystals protruding above the surface.

Table 6

SCALE DESCRIPTION

	738 Inconel Y Doped	738 Inconel Undoped
Spallation	No spallation detected after 50 hr. oxidation in air at 1000°C.	No spallation detected after 50 hr. oxidation in air at 1000°C.
Thickness	Internal oxidation layer 10-12 μm with elongated continuous shape.	Internal oxidation layer 7-9 μm. Slightly elongated, non-continuous shape
Morphology	Fine crystalline structure	Fine crystalline structure. Crystals slightly bigger than those found for the doped sample. In a few places evidence of coagulation to bigger groups.

Table 7

TEST RESULTS OF YTTRIUM DOPED, MODIFIED 304SS

YTTRIUM DOPED ALLOY	Number of 20 Hours, 1000°C Cycles in Air 1 2 3 4 5 6 7 8 9 10 11 12 13 14 15 16 17 18 19 20
304SS without Mn or Si	Fe_2O_3 Scale Spalled
304SS with Mn without Si	Fe_2O_3 Scale Spalled
Commercial 304SS with Mn and Si	Cr_2O_3 Scale Formed ——— Fe_2O_3 Scale Spalled
304SS with Si without Mn	Cr_2O_3 Scale Formed ——— TEST DISCONTINUED SCALE UNSPALLED

Table 8

ISOTHERMAL TEST RESULTS (1000°C) YTTRIUM DOPED, MODIFIED 304 SS

Material:	"pure" 304SS without Mn without Si	"+Mn" 304ss with Mn without Si	"comm." 304SS with Mn with Si	"+Si" 304SS without Mn with Si
Behavior:	spalled in 9 hours	spalled in less than 20 hours	unspalled in 50 hours test discontinued	unspalled in 42 days test discontinued

Table 9

COMPARISON OF DOPED AND UNDOPED MODIFIED 304SS AND COMMERCIAL 304 SS

TESTS	Undoped		Doped	
	"+Si" 304SS without Mn with Si	Commercial 304SS with Mn with Si	"+Si" 304SS without Mn with Si	Commercial 304SS with Mn with Si
20 hour 1000°C Cycles	unspalled after 20 cycles test discontinued	spalled after one cycle	unspalled after 20 cycles test discontinued	spalled after 8-9 cycles
Isothermal 1000°C	unspalled after 42 days test discontinued	spalled in less than 20 hours	unspalled after 42 days test discontinued	unspalled after 50 hours test discontinued

Table 10 Linear Thermal Expansion for Several Oxides (12)

Oxide	Linear Expansion $\Delta L/L_0$ at 1000°C in Different Directions			Linear Expansion Polycrystalline $\Delta L/L_0$ at 1000°C
Y_2O_3	0.823			0.823
CeO_2	1.223			1.223
CaO	1.161			1.161
	c axis	a axis	b axis	
La_2O_3	1.577	0.979	-	1.170
Cr_2O_3	0.663	0.831	-	0.775
HfO_2	1.184	0.826	0.150	0.721
ZrO_2	1.270	0.810	0.141	0.738

Table 11

Liquidus Temperatures (°F) for Selected Oxide Combinations(13)

	Al_2O_3	BeO	CaO	CeO_2	Cr_2O_3	MgO	SiO_2	ThO_2	TiO_2	ZrO_2	Spinel	Zircon
Al_2O_3	3720											
BeO	3450	4580										
CaO	2550	2640	4660									
CeO_2	3180	3580	3630	4980								
Cr_2O_3	3720	4030	1870	4080	4110							
MgO	3470	3270	4160	3990	3850	5070						
SiO_2	2810	3040	2620	3090	3090	2800	3110					
ThO_2	3180	3900	4160	4710	3230	3810	3090	5520				
TiO_2	3130	3090	2590	2730	3180	2910	2800	2960	3320			
ZrO_2	3090	3630	3990	4350	4220	2730	3050	4850	3180	4890		
$MgO \cdot Al_2O_3$	3470	~3130	~3360	~3090	~3450	3680	2450	~3180	2910	3880	~3880	
$ZrO_2 \cdot SiO_2$	2800	~3000	~2550	~3090	~3090	~2730	3050	~3060	2730	3050	2370	4390

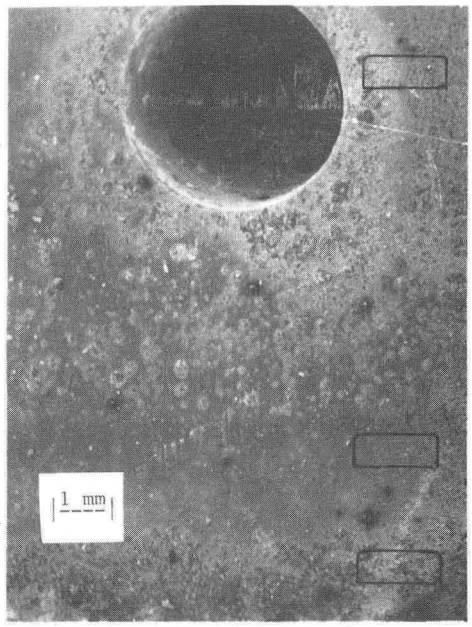

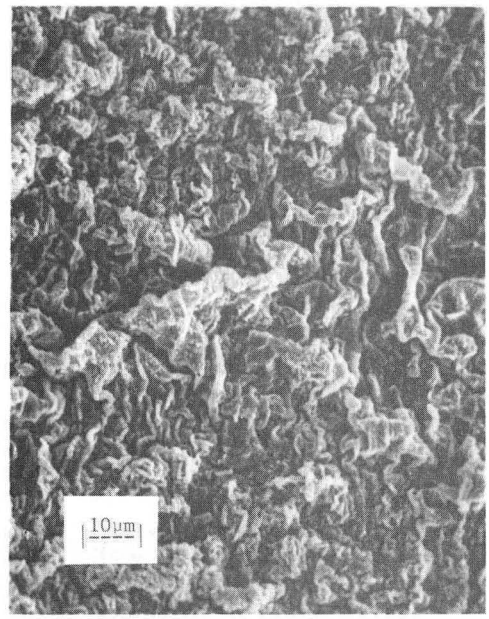

a

b

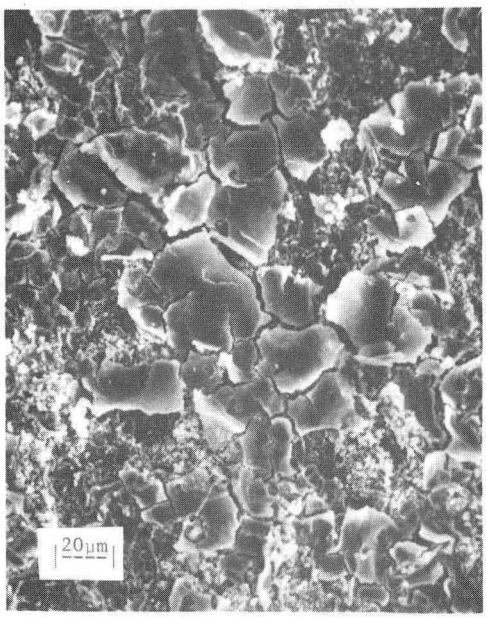

"+Si" 304SS
with Si
without Mn
2 x 20 hours
1000° cycles

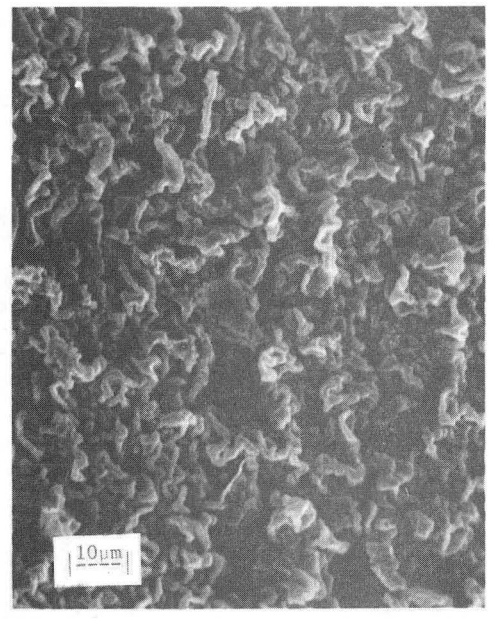

c

b

Fig. 1. Yttrium doped 304SS showing non-uniformities of surface morphology at different places along the sample

XBB 831-10073

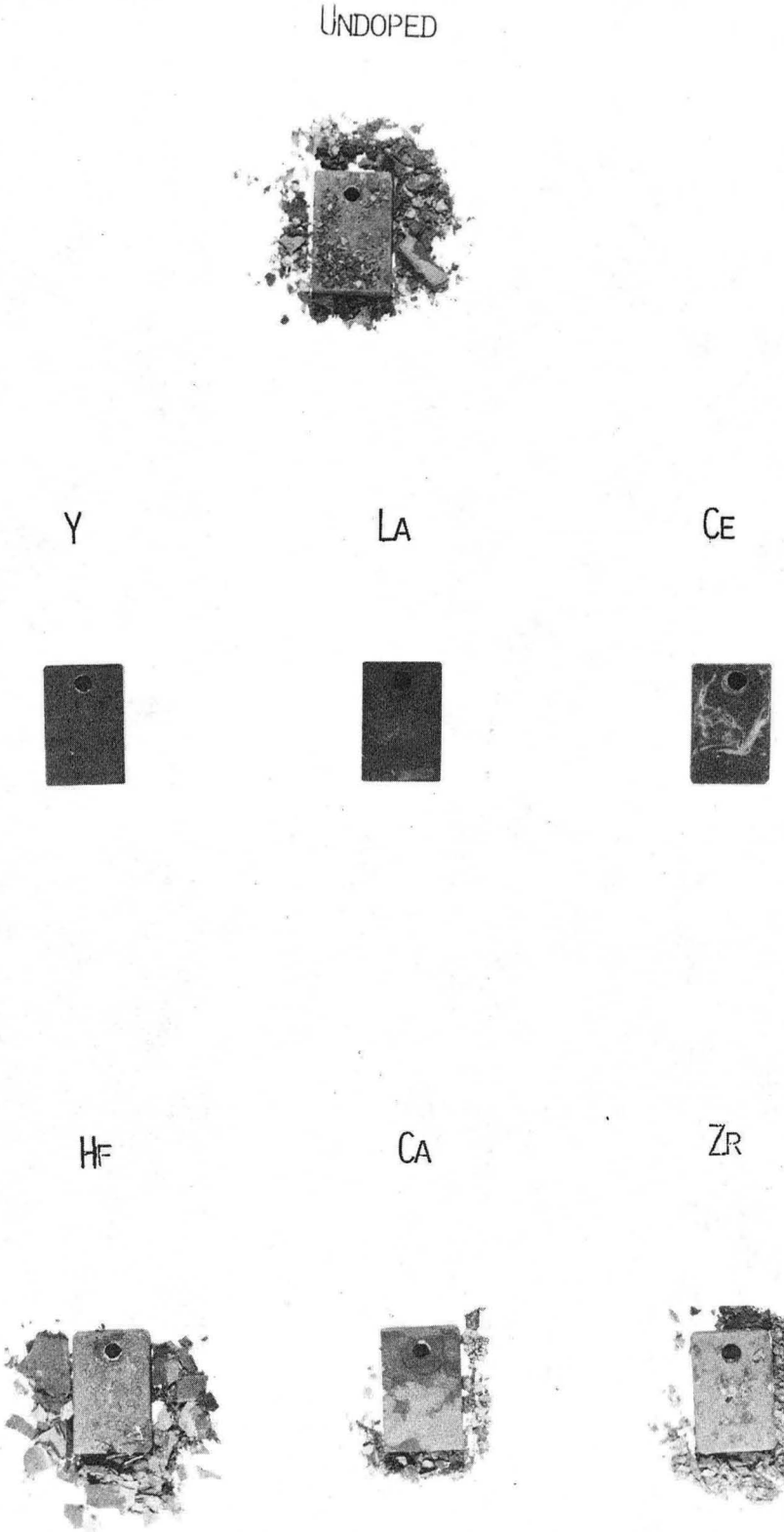

Fig. 2. 304SS alloy doped with different active elements after isothermal oxidation

XBC 803-3113

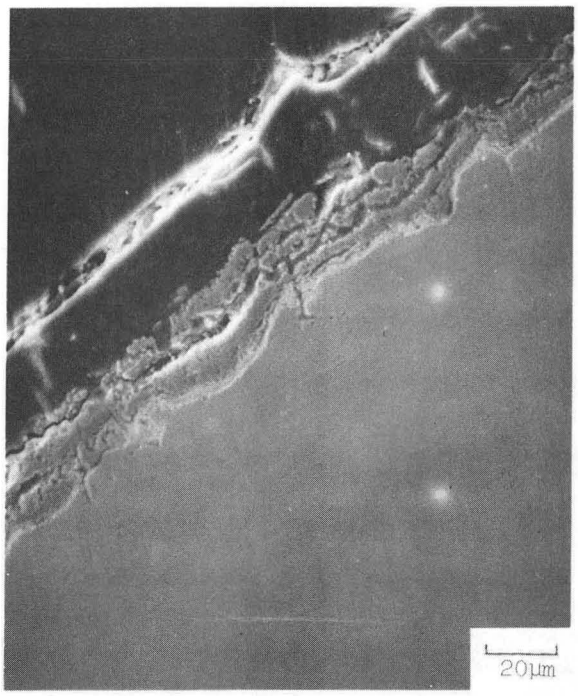

Cr Map

Fe Map

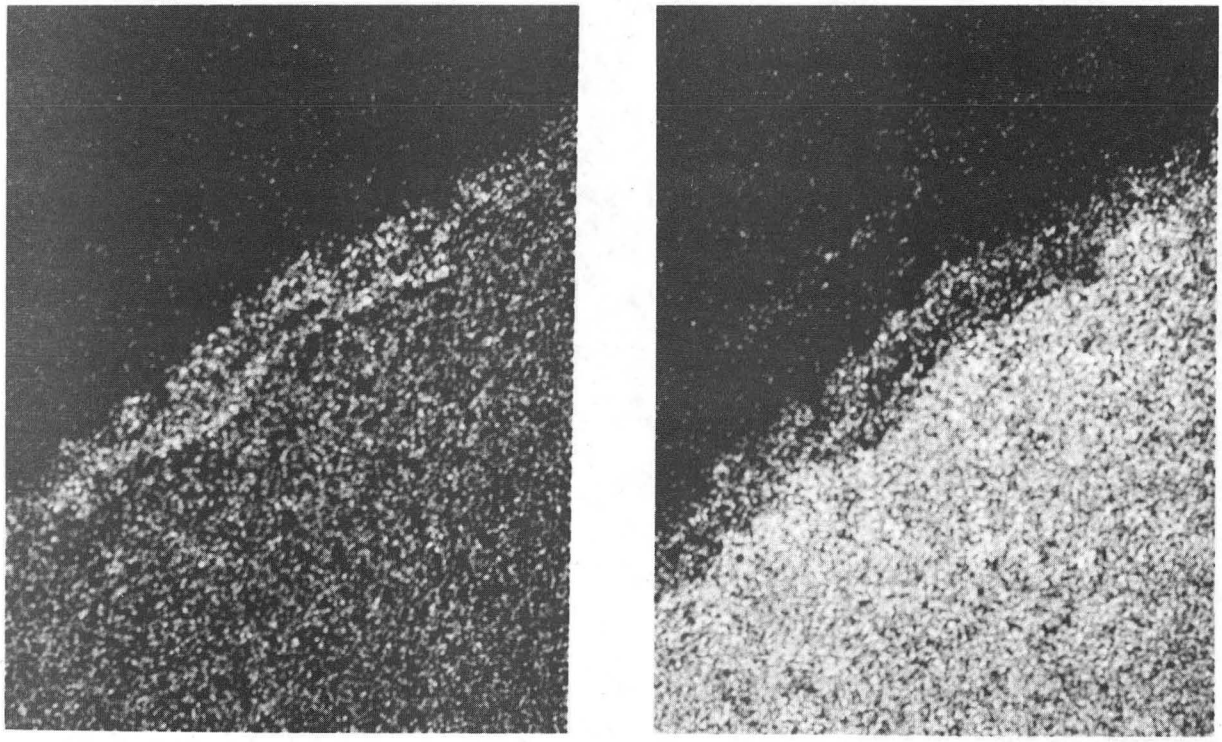

XBB 805-6208

Fig. 3 Cross section of the 304SS undoped sample oxidized for 50 hr at 1000°C in air

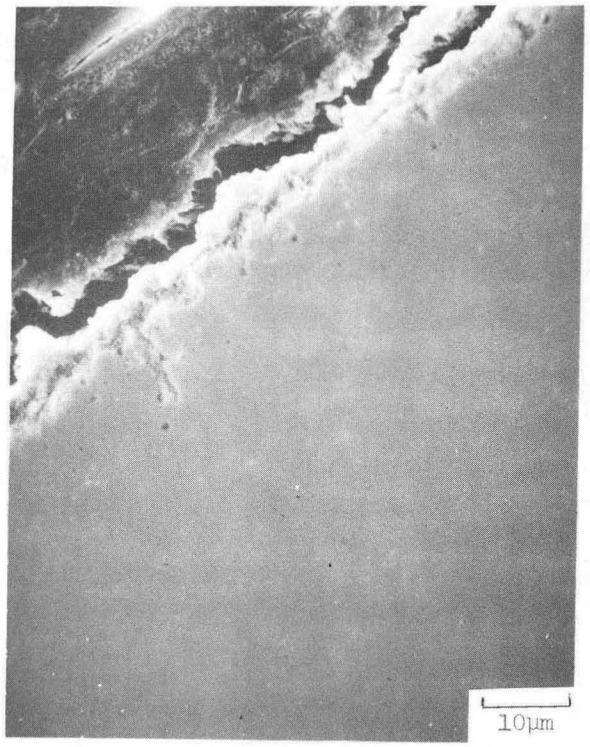

Cr Map

Fe Map

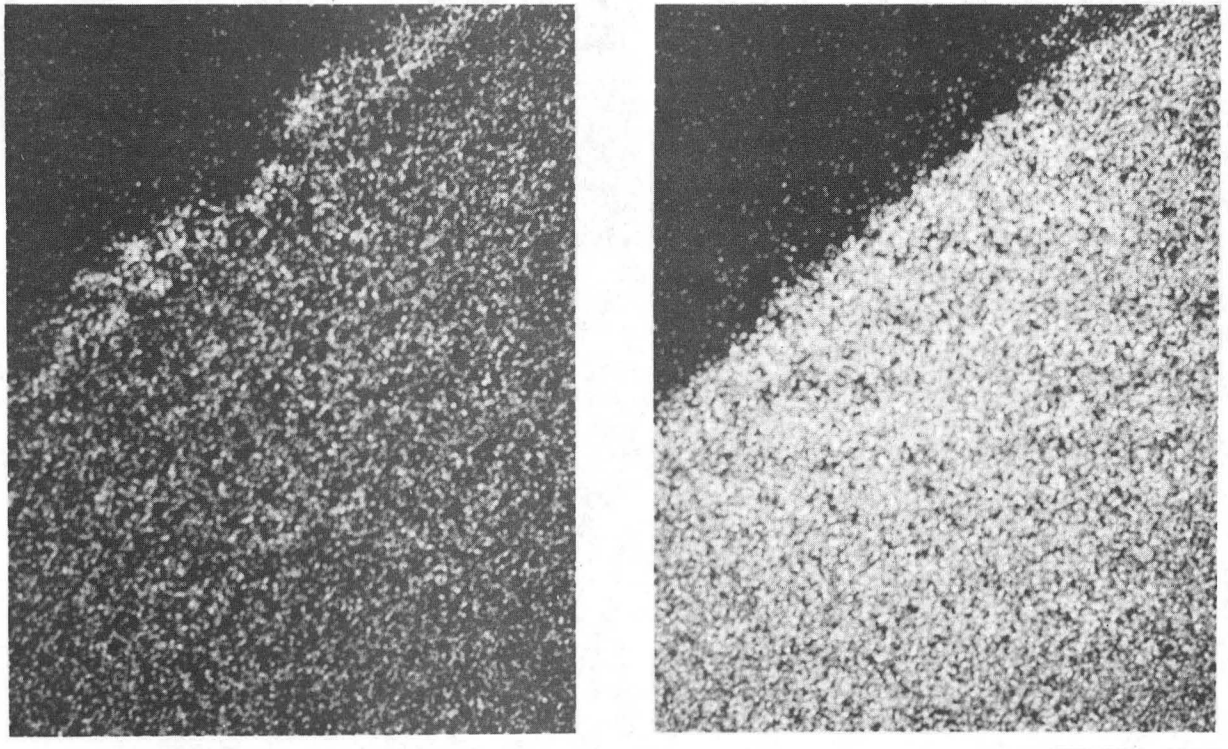

XBB 805-6209

Fig. 4 Cross section of the 304SS yttrium doped sample oxidized for 50 hr at 1000°C in air

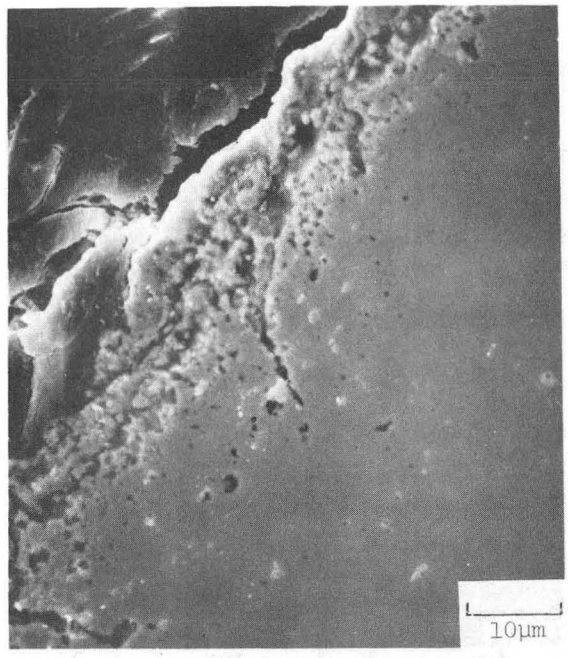

Cr Map

Fe Map

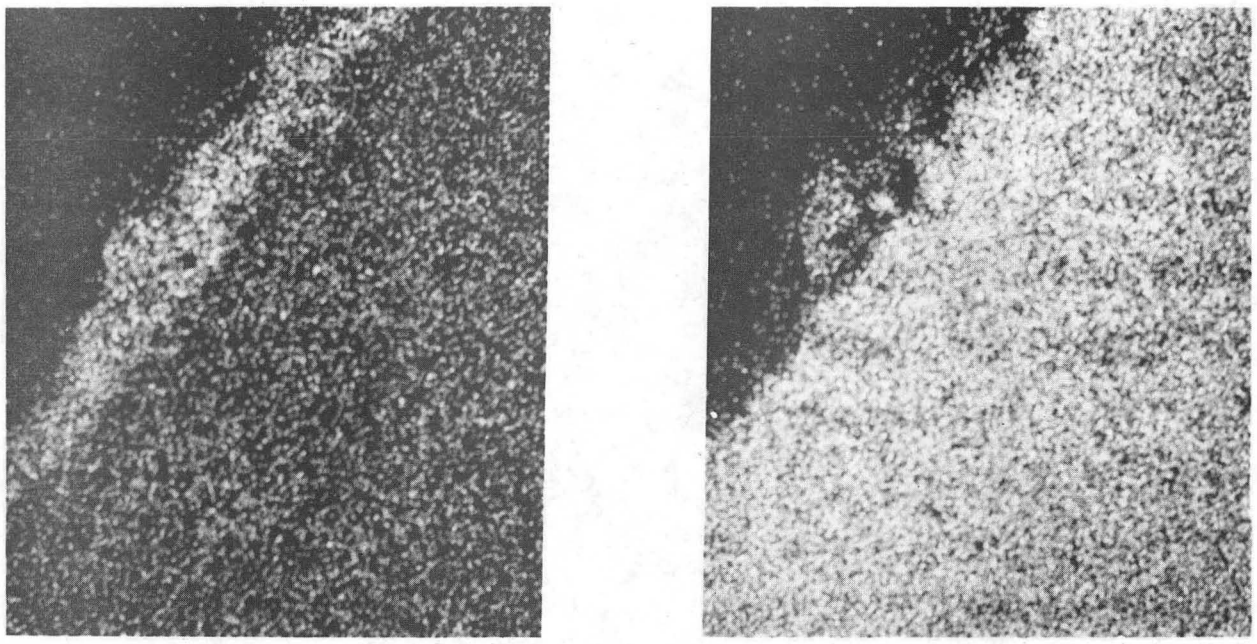

XBB 805-6210

Fig. 5 Cross section of the 304SS cerium doped sample oxidized for 50 hr at 1000°C in air

a

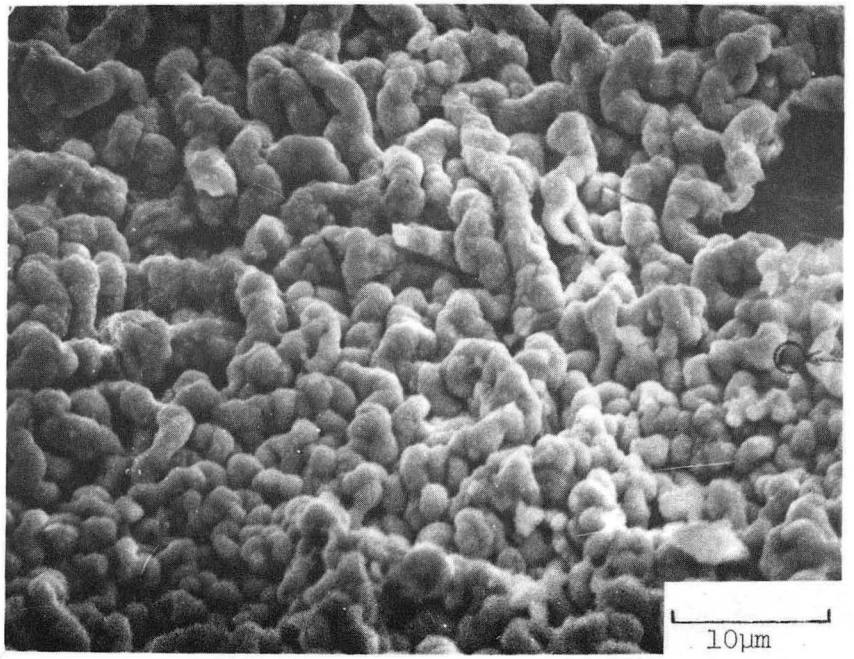

b

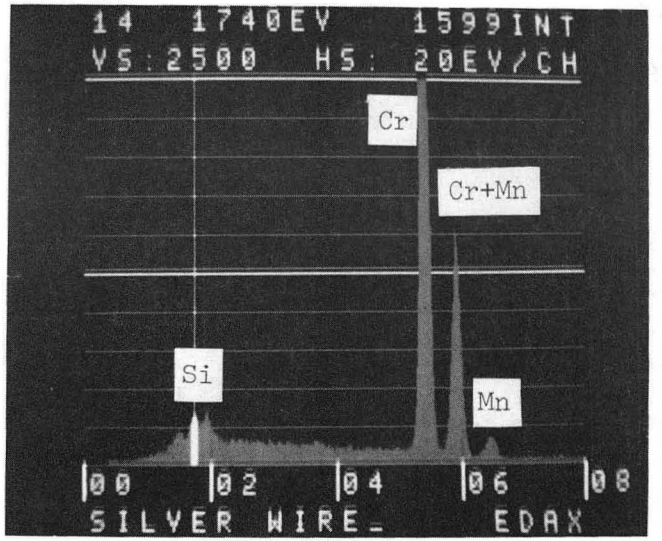

XBB 805-6200

Fig. 6 Outer surface of 304SS yttrium doped oxide scale removed from the substrate

a

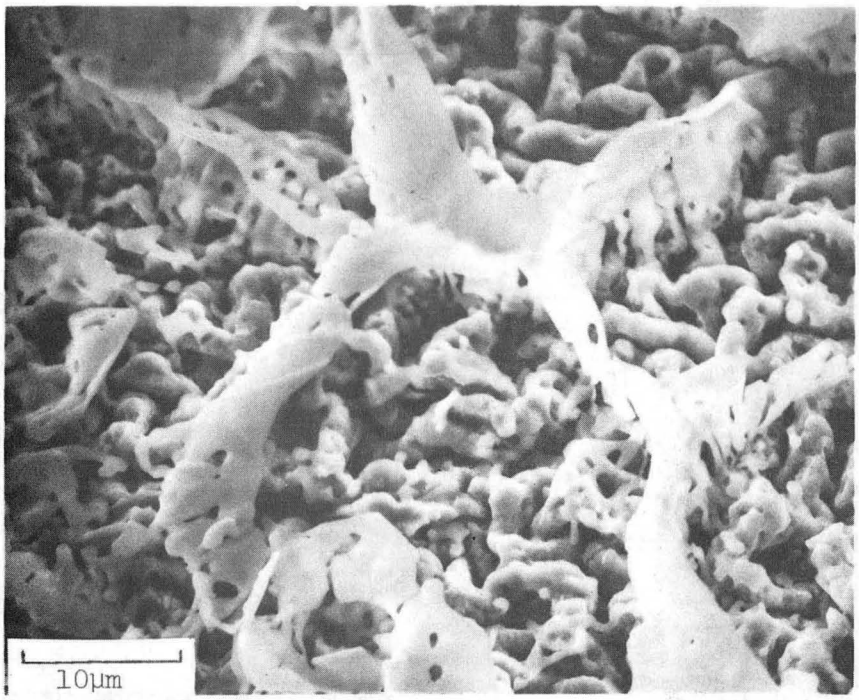

b

Si Map

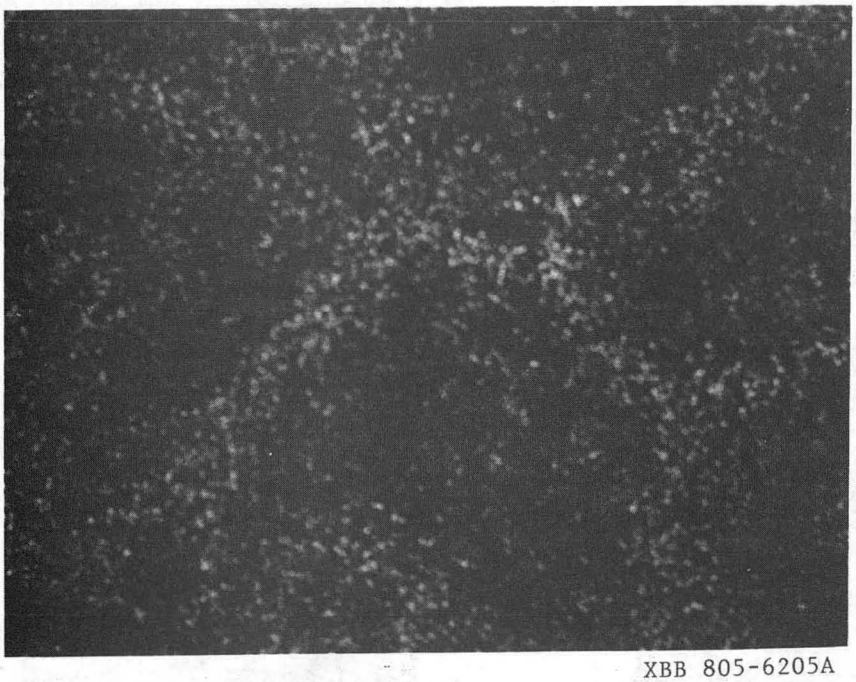

XBB 805-6205A

Fig. 7 Under surface of the 304SS yttrium doped oxide scale removed from the substrate

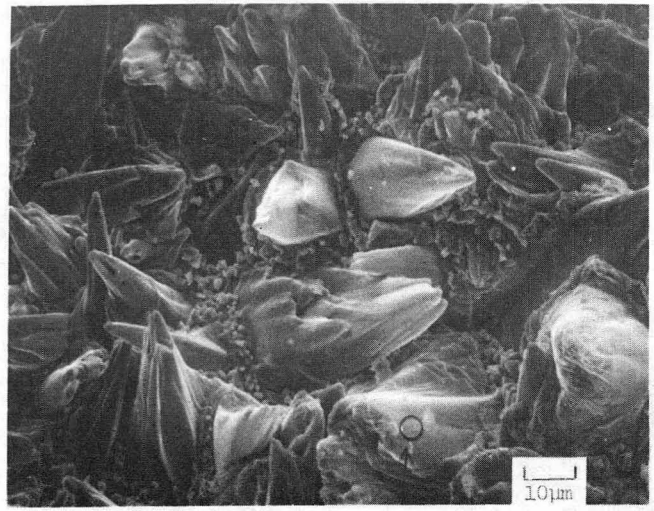

Outer Surface

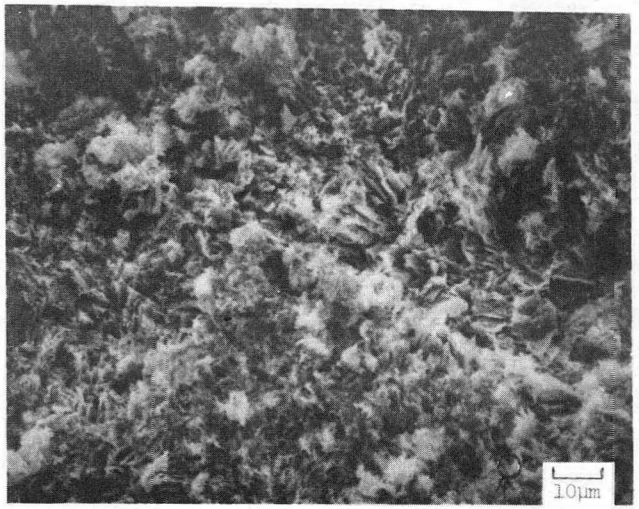

Under Surface

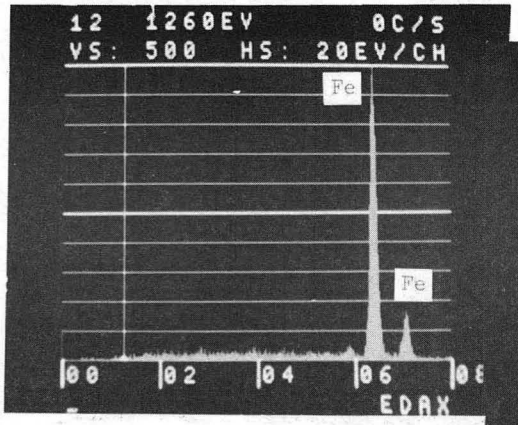

Outer Surface Protrusion

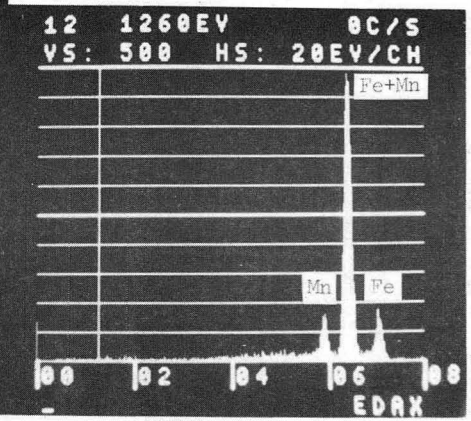

Outer Surface Matrix

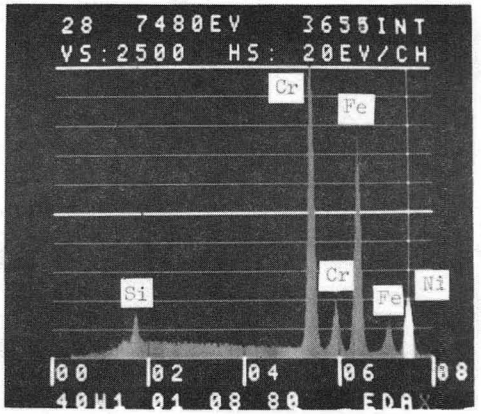

Under Surface

XBB 805-6206

Fig. 8 Outer (a) and under (b) surface of the 304SS undoped, spalled off oxide scale

a

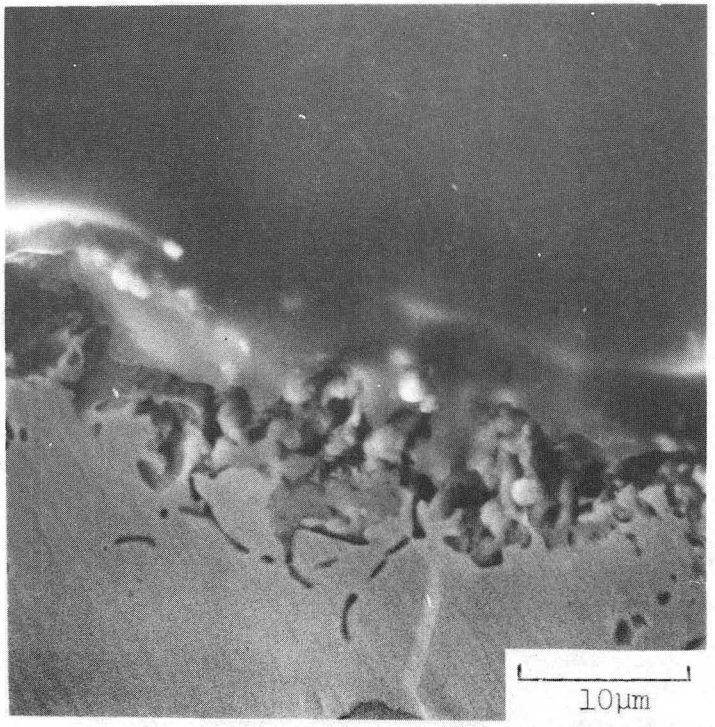

Doped with Y

b

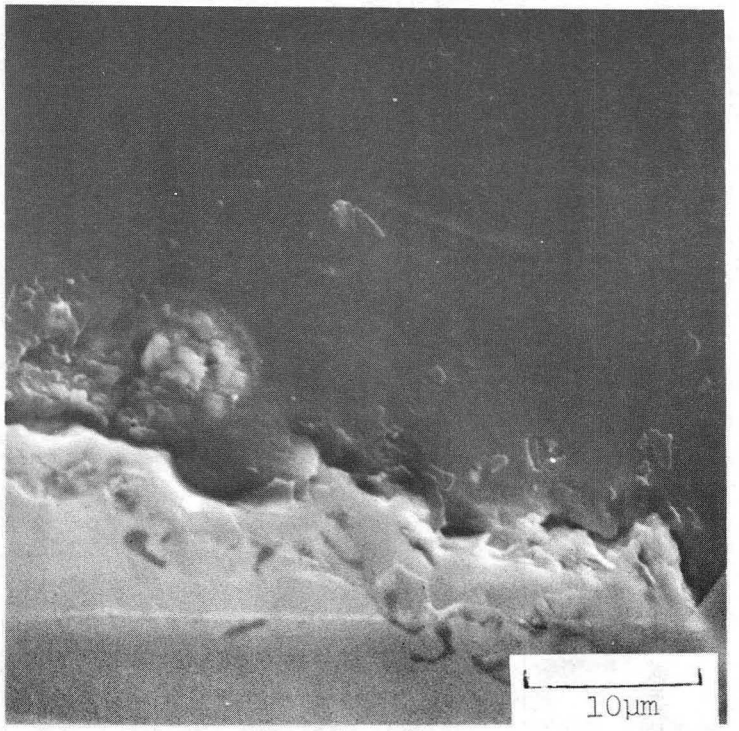

XBB 805-6201

Undoped

Fig. 9 Cross-section of the 310SS yttrium doped and undoped samples oxidized for 50 hr at 1000°C in air

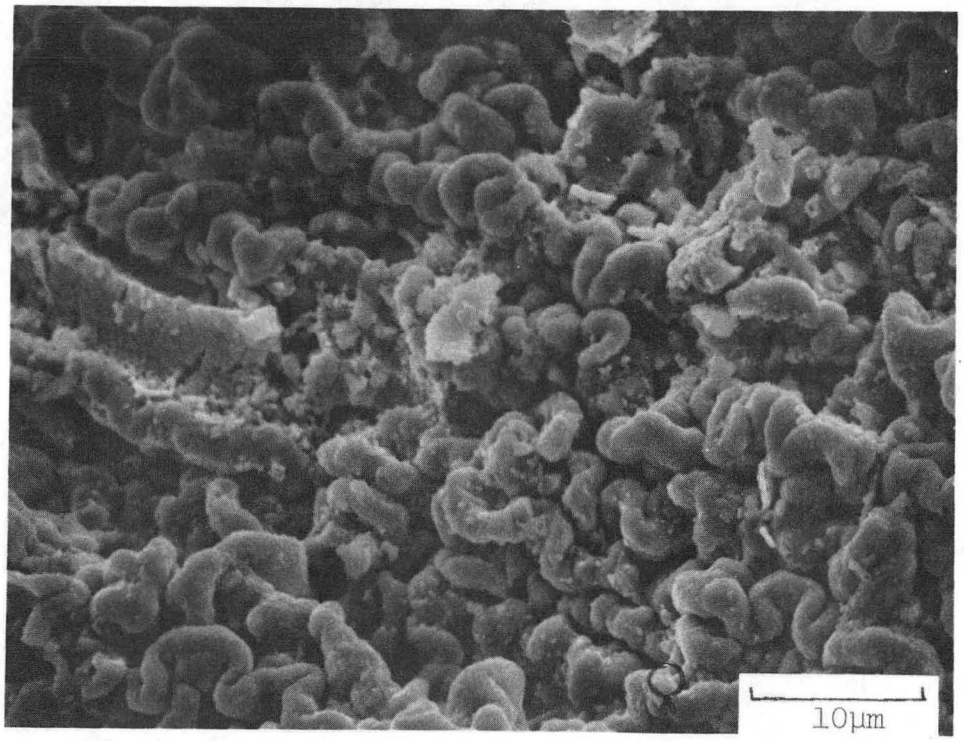

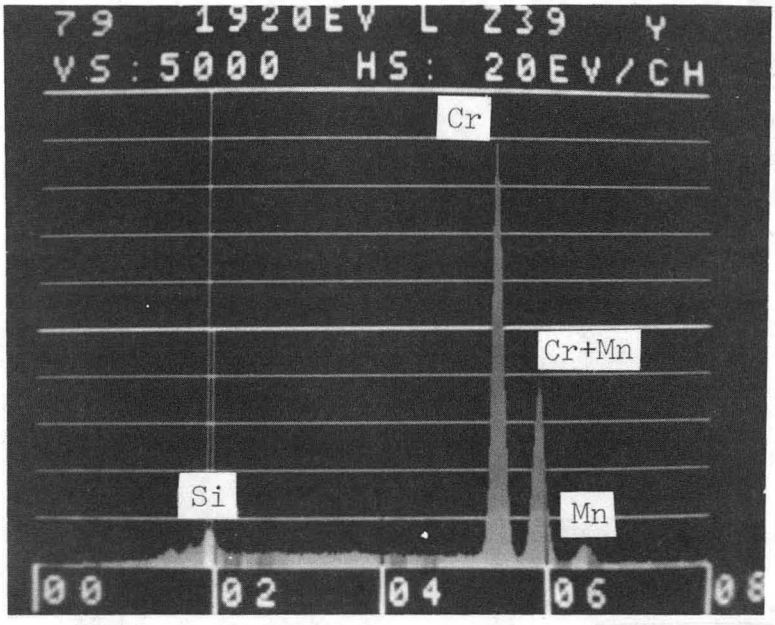

XBB 805-6203

Fig. 10 Outer surface of the 310SS yttrium doped oxide scale

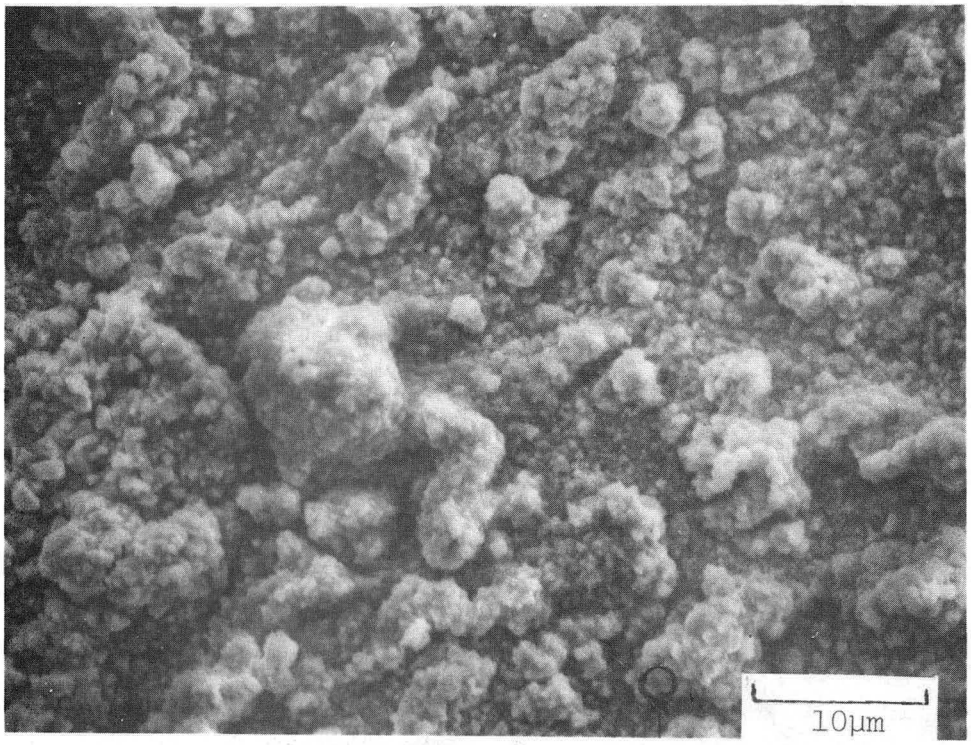

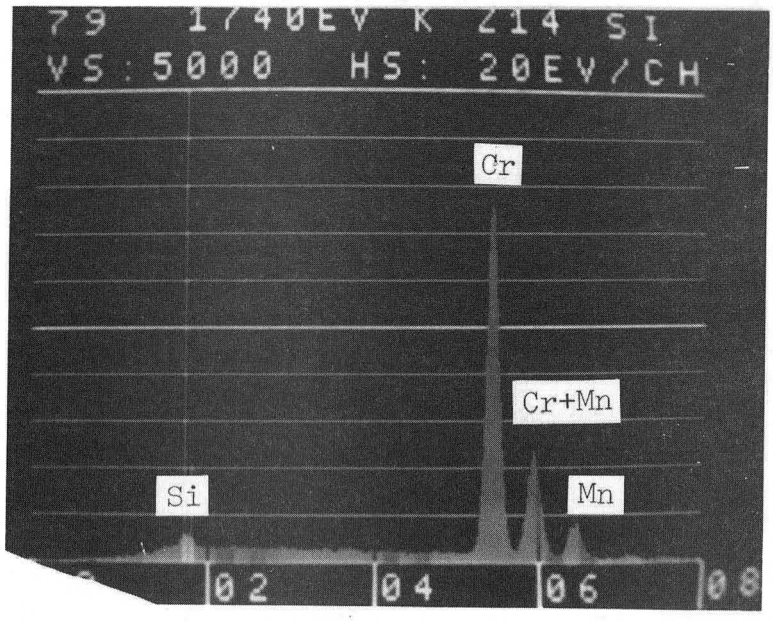

XBB 805-6204

Fig. 11 Outer surface of the 310SS undoped stripped off oxide scale

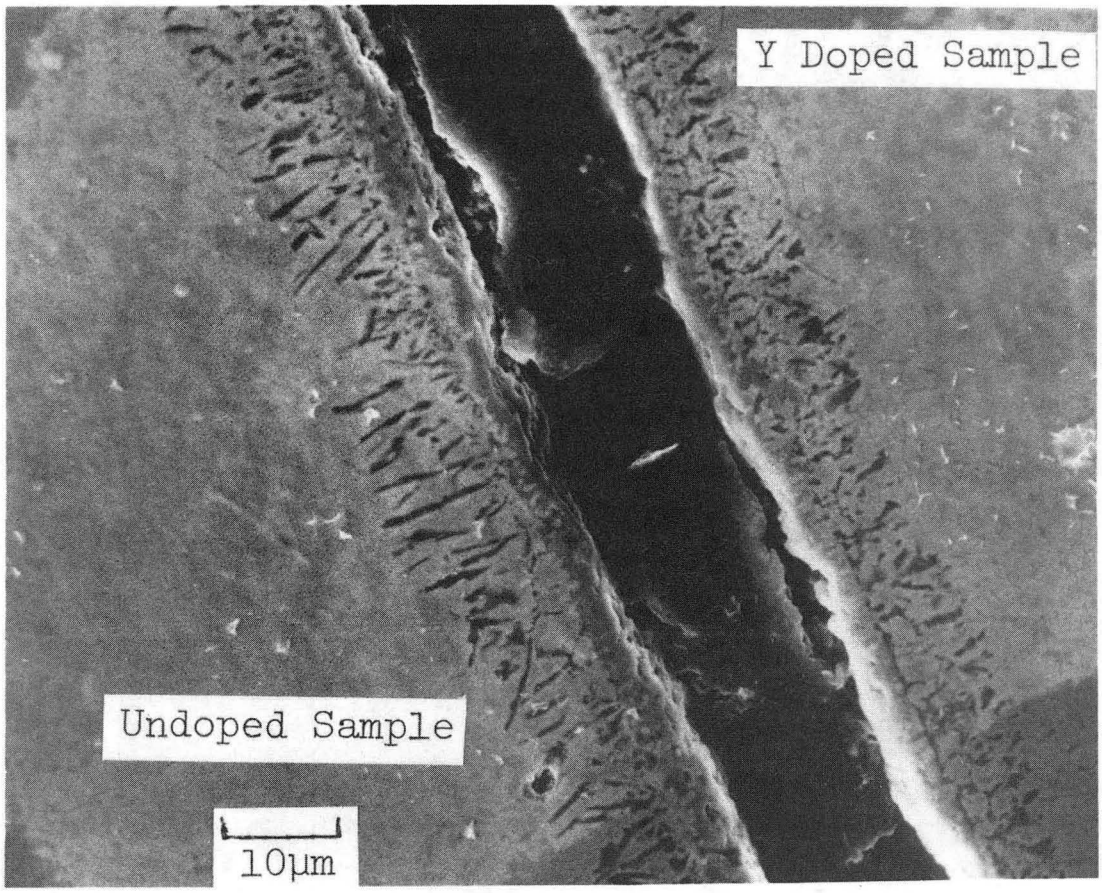

XBB 805-6202

Fig. 12 Cross section of the 738 Inconel alloy yttrium doped and undoped samples oxidized for 50 hours at 1000°C in air

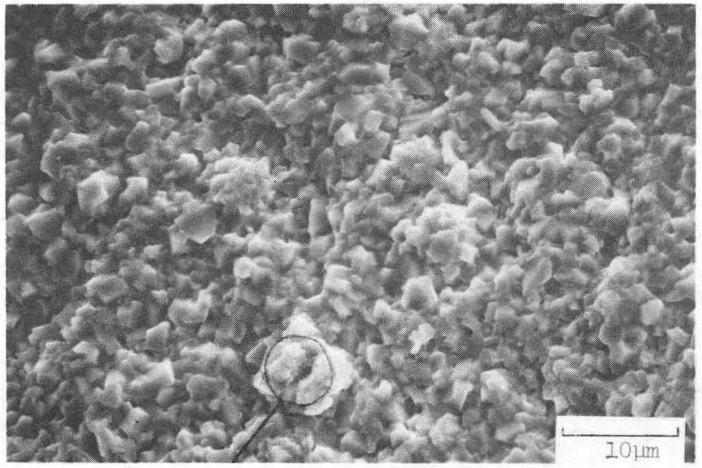

A Undoped Sample

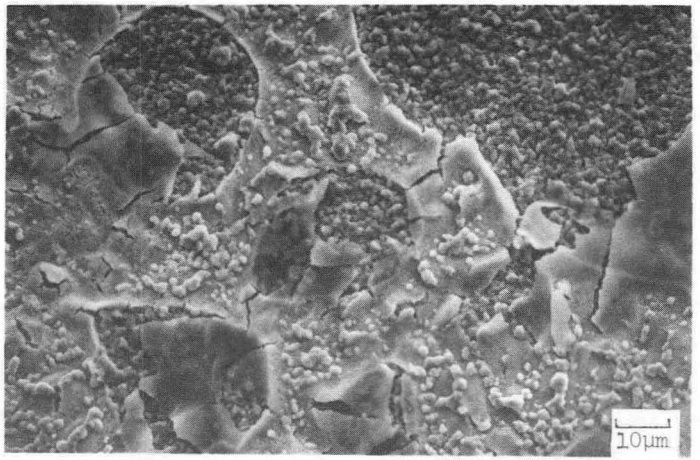

B Doped Sample

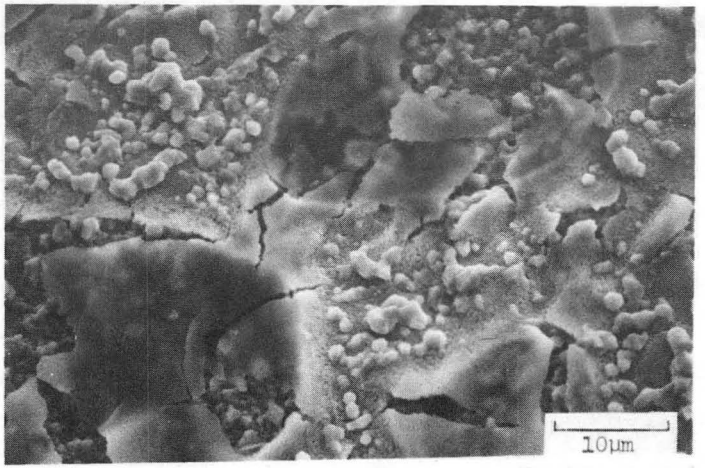

XBB 805-6207

B Doped Sample

Fig. 13 Outer surface of the IN-738 Yttrium doped (a) and undoped (b) stripped off oxide scale

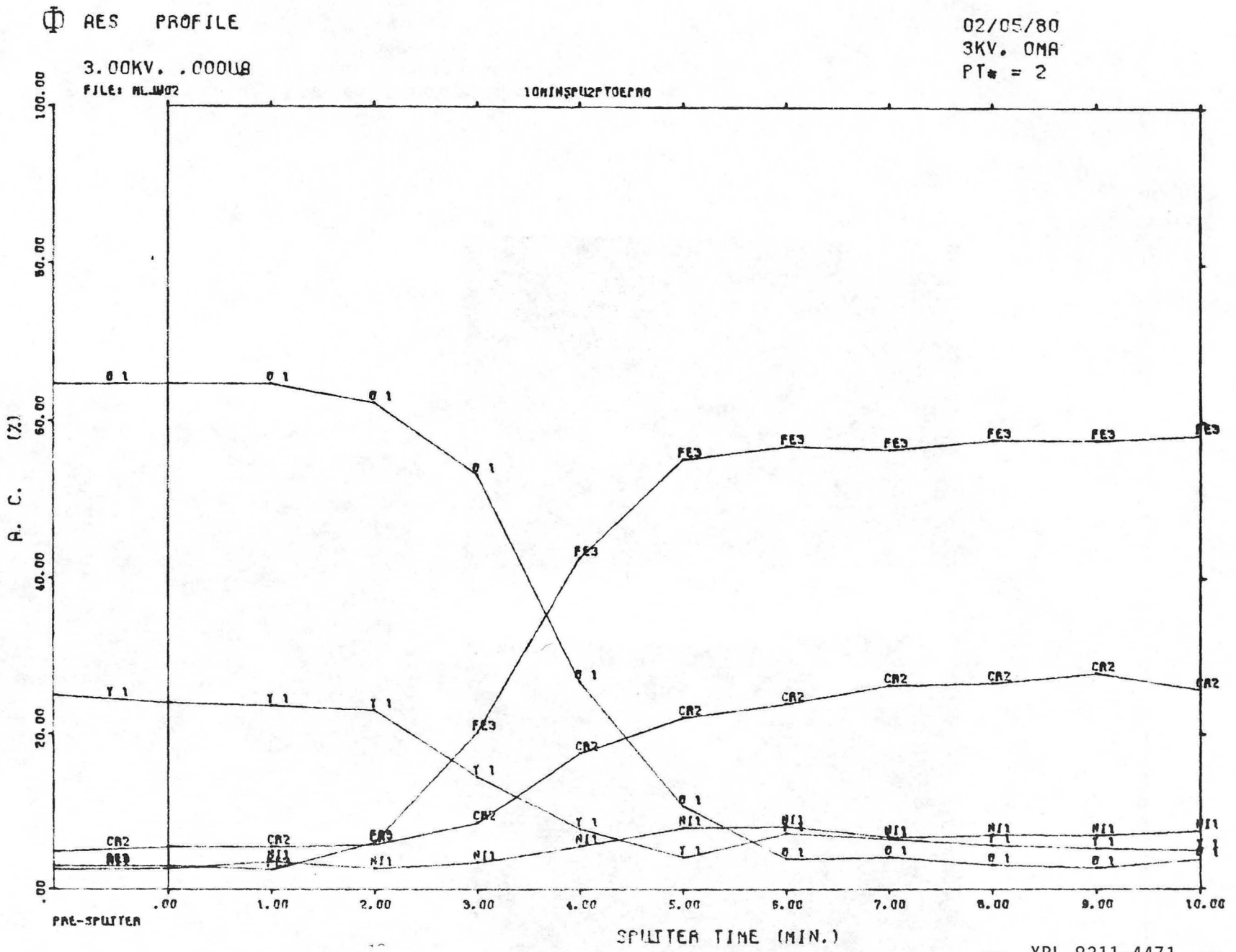

-- XBL 8311-4471 --

Fig. 14 SAM composition profile through the oxide scale on 304SS yttrium doped sample after the preoxidation stage (30 min. at 500°C). Sputtering rate ~400 Å/min

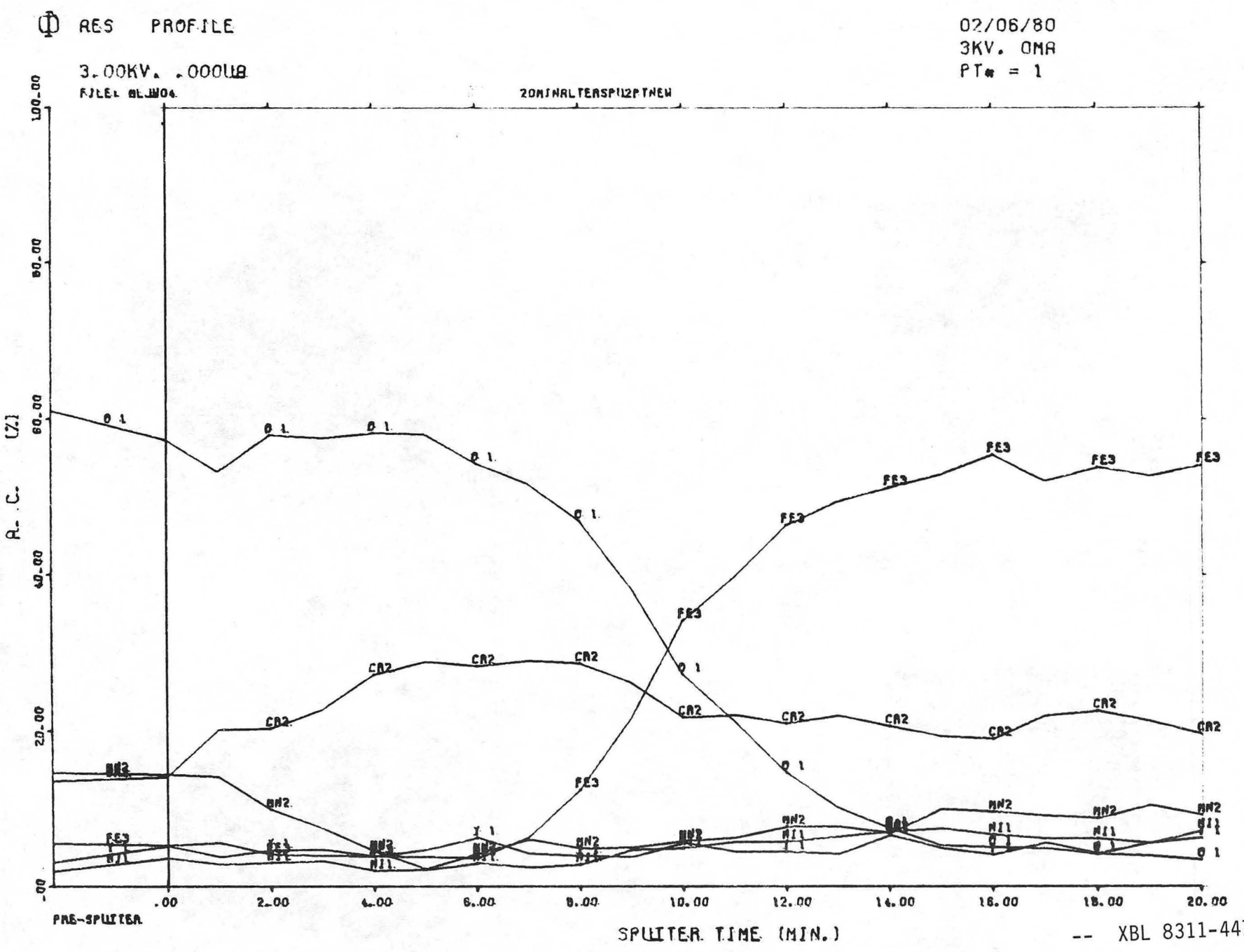

Fig. 15 SAM composition profile through the oxide scale formed on 304SS yttrium doped sample after the preoxidation (30 min. at 50°C) + oxidation (15 min. at 1000°C stage. Sputtering rate ~400 Å/min.

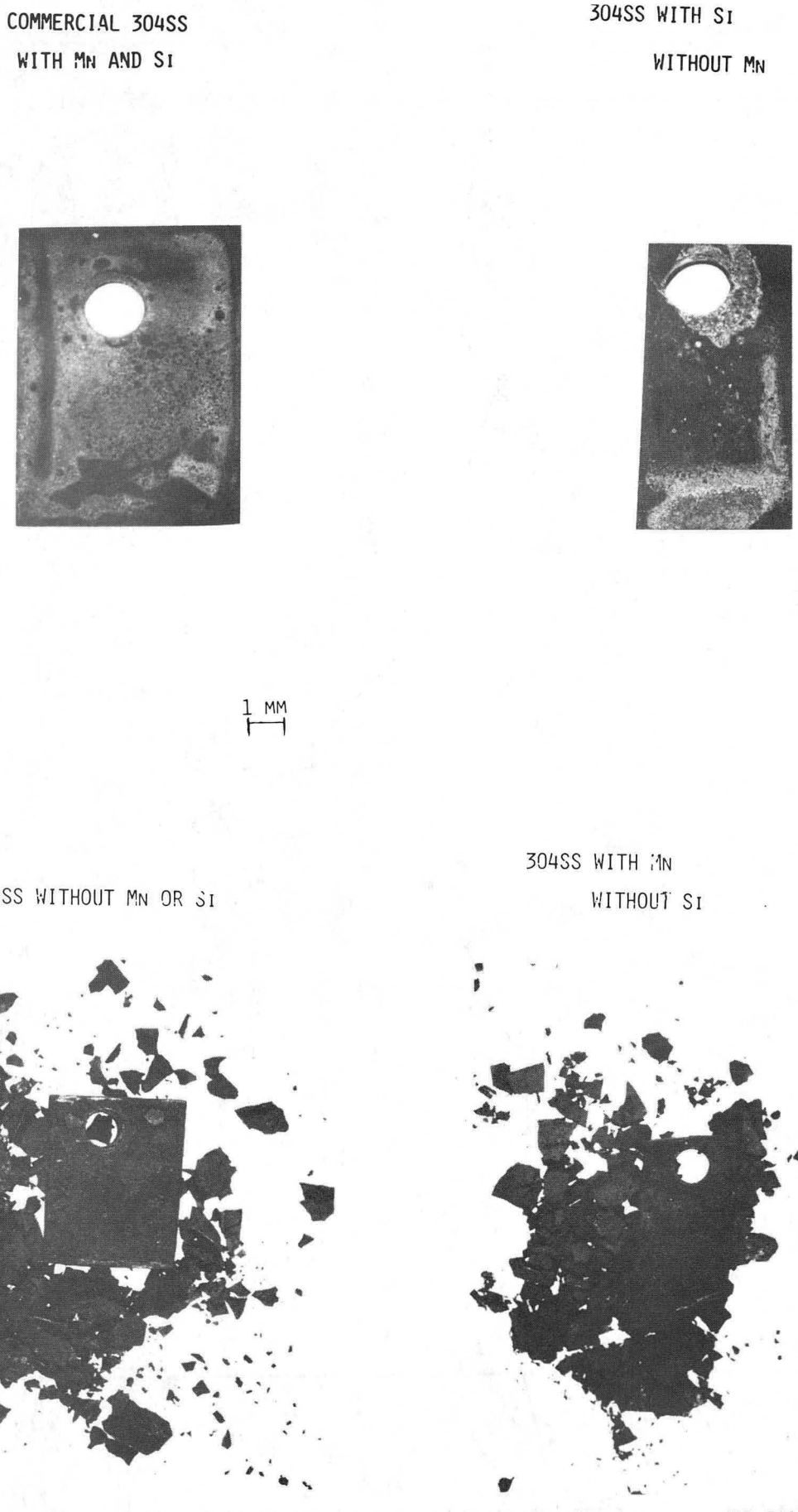

Fig. 16 Yttrium doped alloy modifications of 304SS shown after oxidation exposure

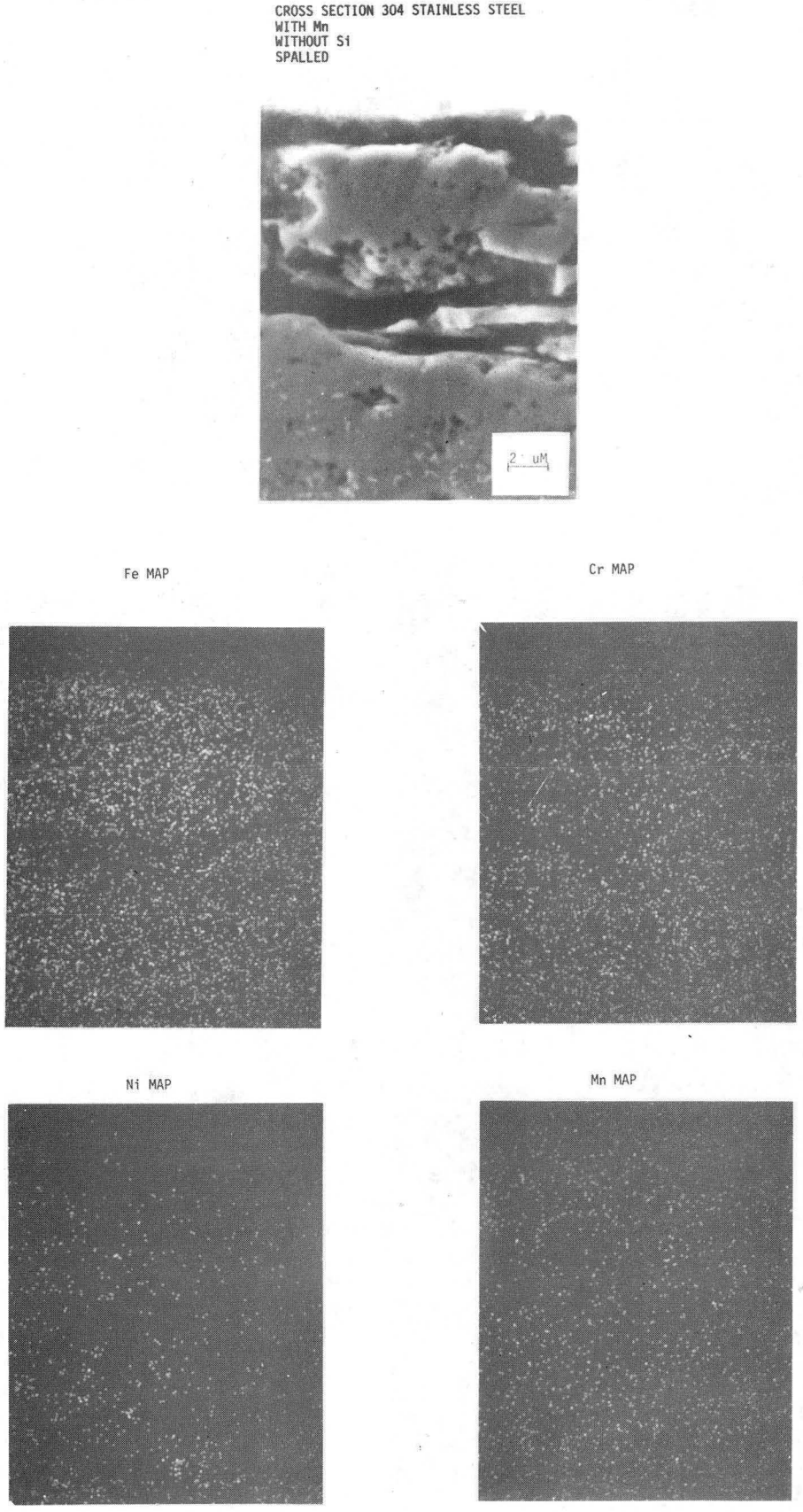

Fig. 17 Cross section of modified (with Mn without Si) 304SS in the spalled condition

XBB 823-1818

CROSS SECTION 304 STAINLESS STEEL
WITH Si
WITHOUT Mn
UNSPALLED

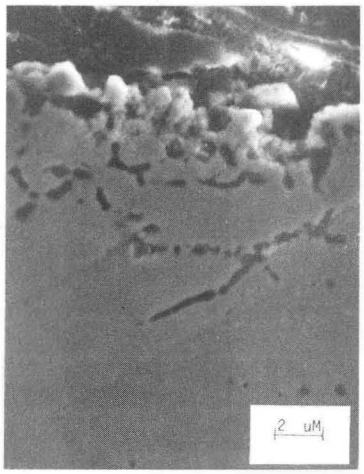

Fe MAP

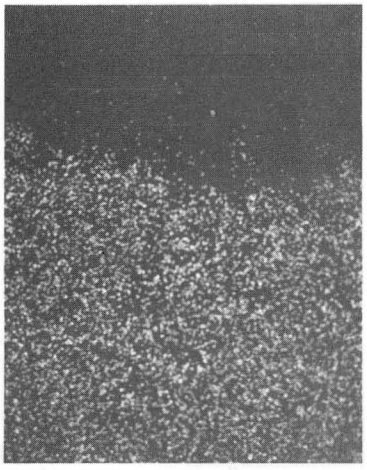

Cr MAP

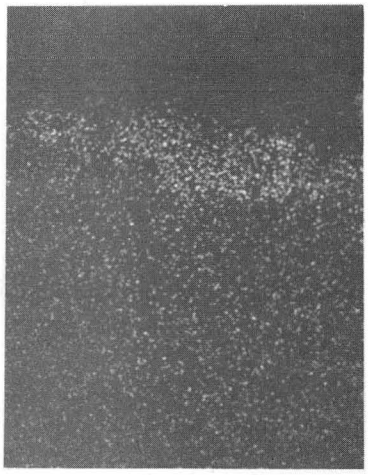

Ni MAP

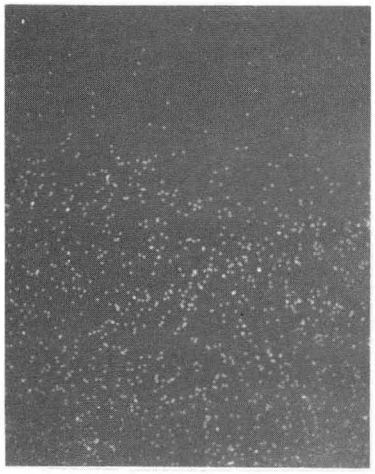

Si MAP

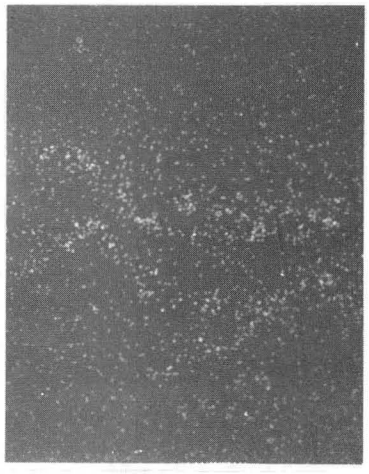

Fig. 18 Cross section of modified (with Si without Mn) 304SS in the unspalled condition

XBB 823-1819

304SS Samples doped with YNO_3

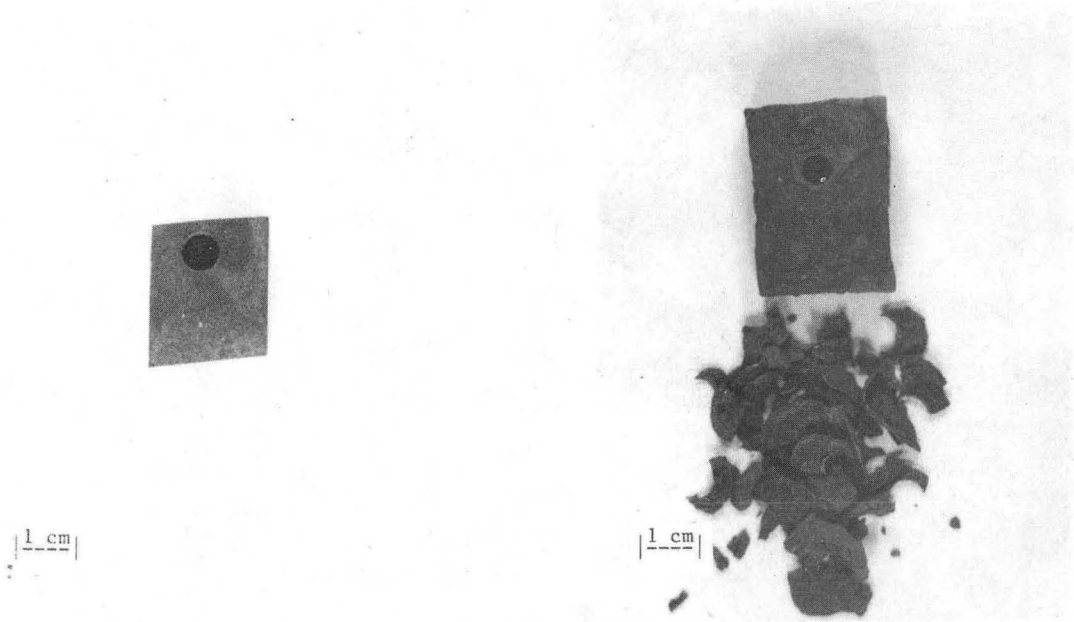

XBB 8311-10042

"+Si" 304SS
with Si
without Mn
twenty thermal cycles
at 20 hr/1000°C unspalled

Commercial 304SS
with Si
with Mn
ten thermal cycles at
1000°C spalled

Fig. 19 Samples showing the increased high temperature spallation resistance of doped +Si 304SS (no Mn) compared to doped commercial 304SS (Mn+Si)

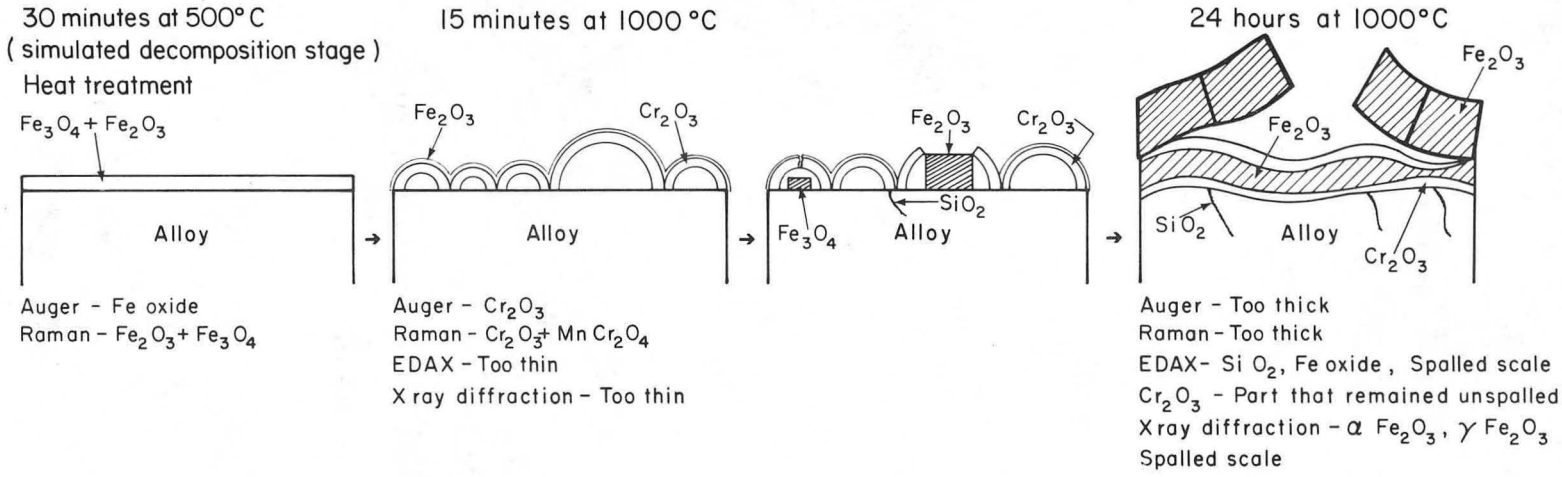

Fig. 20 Proposed corrosion mechanism of undoped commercial 304SS

XBL 809 - 1889

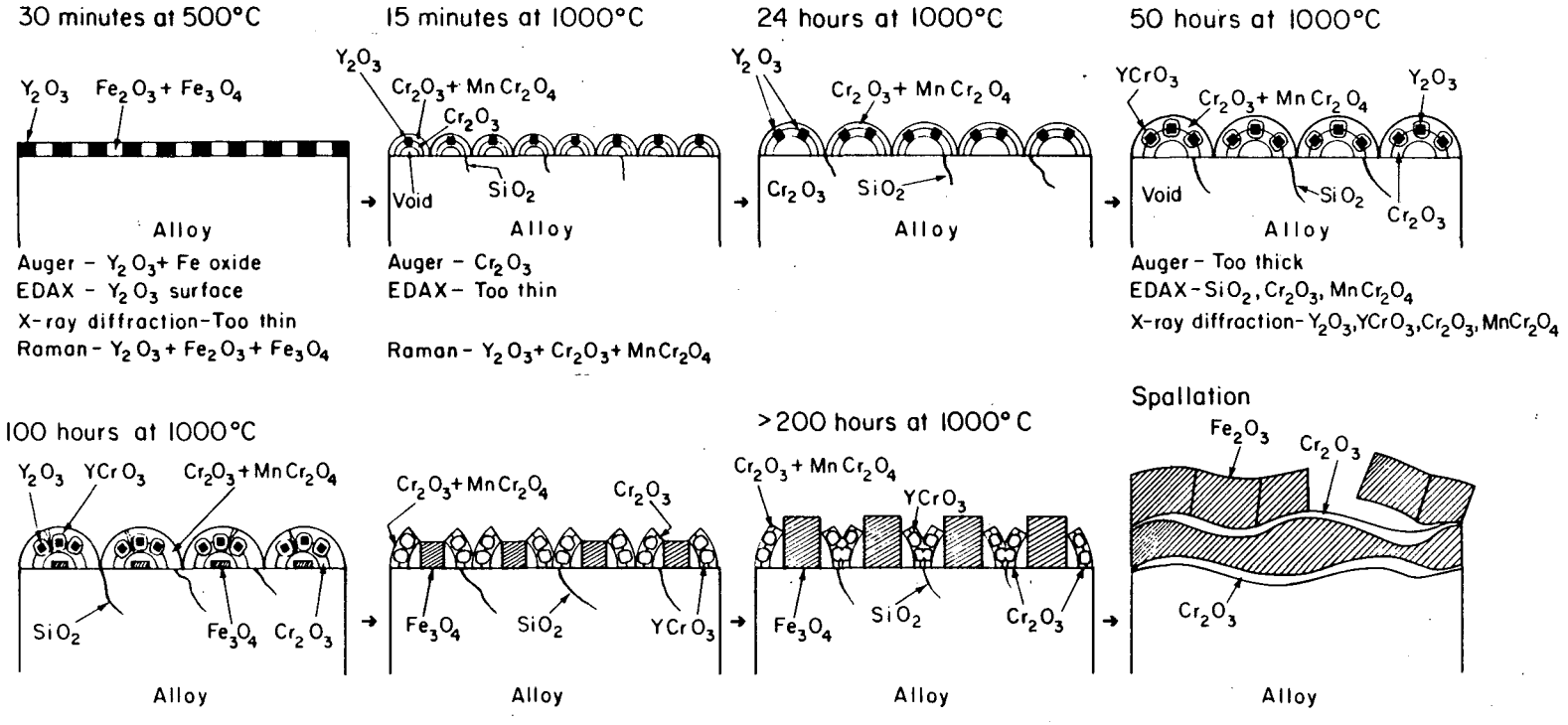

Y-doped 304 stainless steel

Fig. 21 Proposed corrosion mechanism of yttrium doped commercial 304SS

XBL809-1890

DISTRIBUTION LIST

Wate Bakker
EPRI
3214 Hillview Avenue
P.O. Box 10412
Palo Alto, CA 94304

B.R. Banerjee
Ingersoll-Rand Company
P.O. Box 301
Princeton, NJ 08540

K.L. Baumert
Air Products & Chemicals, Inc.
P.O. Box 538
Allentown, PA 18105

S.M. Benford
NASA Lewis Research Center
21000 Brookpark Road
Cleveland, OH 41135

A.E. Biggs
Arco Chemicals
3801 W. Chester Pike
Newtown Square, PA 19073

R. Blickensderfer
Bureau of Mines
P.O. Box 70
Albany, OR 97321

R.A. Bradley, Manager
Fossil Energy Materials Program
Oak Ridge National Laboratory
P.O. Box X
Oak Ridge, TN 37830

Richard Brown
Materials Laboratory
Department of Chemical Engineering
University of Rhode Island
Kingston, RI 02881

DISTRIBUTION LIST cont'd

D.H. Buckley
NASA Lewis Research Center
21000 Brookpark Road
Cleveland, OH 41135

P.T. Carlson, Task Leader
Fossil Energy Materials Program
Oak Ridge National Laboratory
P.O. Box X
Oak Ridge, TN 37830

J. Carpenter
ECUT Program
Oak Ridge National Laboratory
P.O. Box X
Oak Ridge, TN 37830

J.P. Carr
Department of Energy, Office of Fossil Energy
FE-42 Mailstop 3222-GTN
Washington, DC 40525

Hans Conrad
Materials Engineering Department
North Carolina State University
Raleigh, NC 27659

P. Crook
Cabot Corporation
Technology Department
1020 W. Park Avenue
Kokomo, IN 46901

S.J. Dapkunas
Department of Energy, Office of Fossil Energy
Technical Coordination Staff FE-14
Mailstop C-156 GTN
Washington, DC 40525

DOE Technical Information Center
P.O. Box 62
Oak Ridge, TN 37830

W.A. Ellingson
Argonne National Laboratory
9700 South Cass Avenue
Argonne, IL 60439

DISTRIBUTION LIST cont'd

J. Gonzales
GTE
Chemical & Metallurgical Division
Hawes Street
Towanda, PA 18848

Å. Hammarsten
Teknikum
P.O. Box 534, S-751 21
Uppsala
SWEDEN

E. Haycock
Westhollow Research Center
Shell Development Company
P.O. Box 1380
Houston, TX 77001

J.M. Hobday
Department of Energy
Morgantown Energy Technology Center
P.O. Box 880
Morgantown, WV 26505

E.E. Hoffman, Manager
National Materials Program
Department of Energy
Oak Ridge Operations
P.O. Box E
Oak Ridge, TN 37830

J.A.C. Humphrey
Mechanical Engineering Department
University of California
Berkeley, CA 94720

I.M. Hutchings
University of Cambridge
Department of Metallurgy
Pembroke Street
Cambridge
ENGLAND

Sven Jansson
Stal-Laval Turbin AB
Finspong S-61220
SWEDEN

DISTRIBUTION LIST cont'd

R.R. Judkins
Fossil Energy Materials Program
Oak Ridge National Laboratory
P.O. Box X
Oak Ridge, TN 37830

M.K. Keshavan
Union Carbide Corporation
Coating Services Department
1500 Polco Street
Indianapolis, IN 46224

T. Kosel
University of Notre Dame
Dept. of Metallurgical Engineering
& Materials Science
Box E
Notre Dame, IN 46556

L. Lanier
FMC-Central Engineering Laboratory
1185 Coleman Avenue
Santa Clara, CA 95052

N.H. MacMillan
Pennsylvania State University
167 Materials Research Laboratory
University Park, PA 16802

P.K. Mehrotra
Kennemetal Inc.
1011 Old Salem Road
Greensburg, PA 15601

Ken Magee
Bingham-Williamette Co.
2800 N.W. Front Avenue
Portland, OR 97219

T. Mitchell
Case Western Reserve University
Department of Metallurgy
Cleveland, OH 44106

Fred Pettit
Dept. of Metallurgy & Materials Engineering
University of Pittsburgh
Pittsburgh, PA 15261

DISTRIBUTION LIST cont'd

R.A. Rapp
Metallurgical Engineering
116 W. 19th Avenue
The Ohio State University
Columbus, OH 43210

D.A. Rigney
Metallurgical Engineering
116 W. 19th Avenue
The Ohio State University
Columbus,OH 43210

A.W. Ruff
Metallurgy Division
National Bureau of Standards
B-266 Materials
Washington, DC 20234

Alberto Sagüés
IMMR - University of Kentucky
763 Anderson Hall
Lexington, KY 40506

Gordon Sargent
University of Notre Dame
Dept. of Metallurgical Engineering & Materials Science
Box E
Notre Dame, IN 46556

Paul Shewmon
Dept. of Metallurgical Engineering
116 W. 19th Avenue
Columbus, OH 43210

Gerry Sorell
EXXON Research & Engineering Company
P.O. Box 101
Florham Park, NJ 07932

John Stringer
University of California
Lawrence Berkeley Laboratory
Mailstop 62/203
Berkeley, CA 94720

Widen Tabakoff
Dept. of Aerospace Engineering
University of Cincinnati
Cincinnati, OH 45221

DISTRIBUTION LIST cont'd

Edward Vesely
IITRI
10 West 35th Street
Chicato, IL 60616

J.J. Wert
Metallurgy Department
Vanderbilt University
P.O. Box 1621, Sta. B
Nashville, TN 37235

J.C. Williams
Dept. of Metallurgy & Materials Science
Carnegie-Mellon University
Schenley Park
Pittsburgh, PA 15213

S. Wolf
Department of Energy
Basic Energy Sciences Office
Division of Materials Sciences
Washington, DC 20545

Ian Wright
Materials Science Division
Battelle Memorial Institute
505 King Avenue
Columbus, OH 43201

C.S. Yust
Metals and Ceramics Division
Oak Ridge National Laboratory
P.O. Box X
Oak Ridge, TN 37830

This report was done with support from the Department of Energy. Any conclusions or opinions expressed in this report represent solely those of the author(s) and not necessarily those of The Regents of the University of California, the Lawrence Berkeley Laboratory or the Department of Energy.

Reference to a company or product name does not imply approval or recommendation of the product by the University of California or the U.S. Department of Energy to the exclusion of others that may be suitable.

TECHNICAL INFORMATION DEPARTMENT
LAWRENCE BERKELEY LABORATORY
UNIVERSITY OF CALIFORNIA
BERKELEY, CALIFORNIA 94720